Towards a Complete Picture of Galactic Star Formation: Theory

Mordecai-Mark Mac Low

Department of Astrophysics

American Museum of Natural History

Initial Mass Function

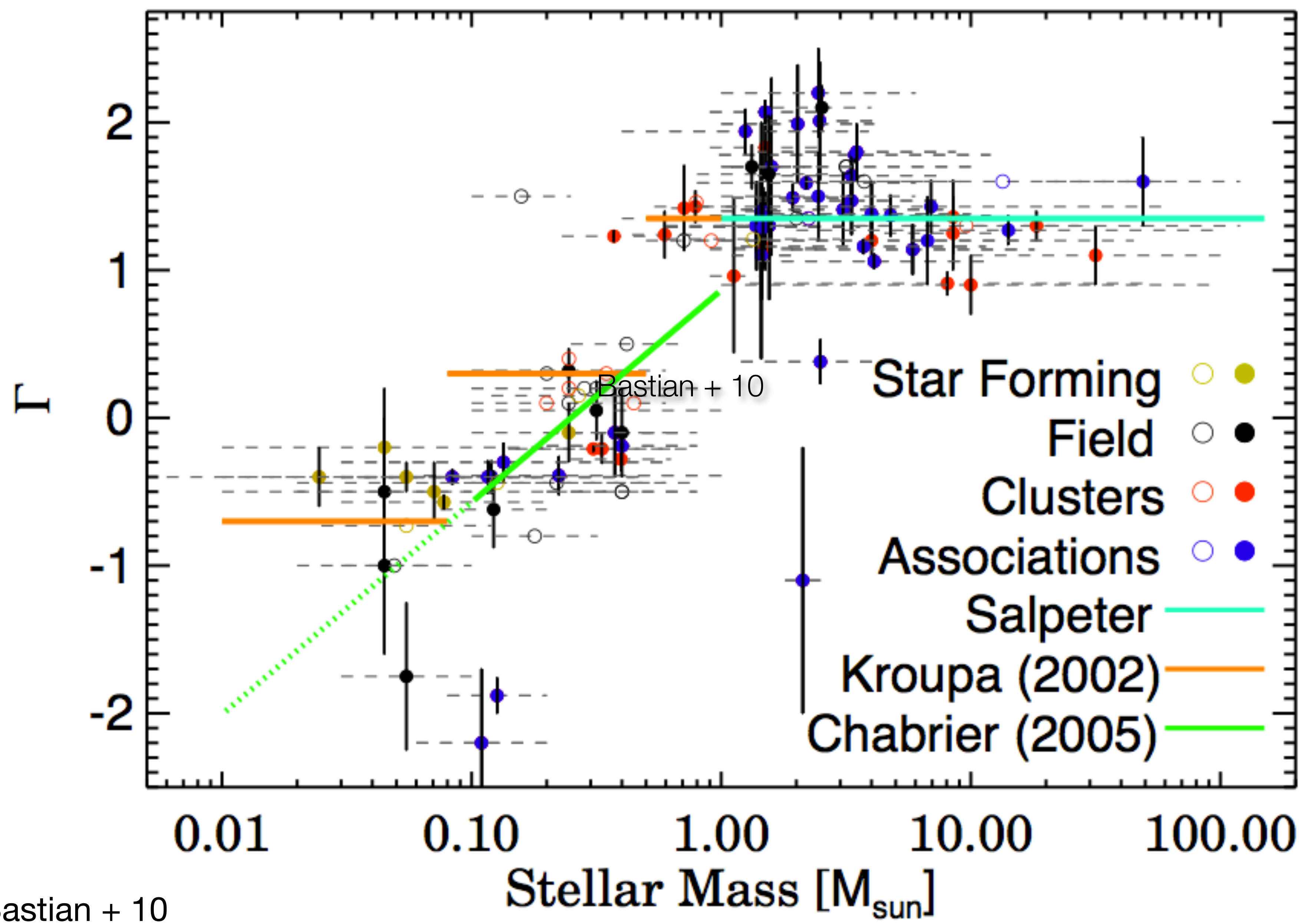

Bastian + 10

Thermodynamics can set the fragmentation scale.

Larson 2005

$$T = 4.4\,\rho_{18}^{-0.27}\,\mathrm{K}, \qquad \rho < 10^{-18}\,\mathrm{g\,cm^{-3}}$$

$$T = 4.4\,\rho_{18}^{+0.07}\,\mathrm{K}, \qquad \rho > 10^{-18}\,\mathrm{g\,cm^{-3}}$$

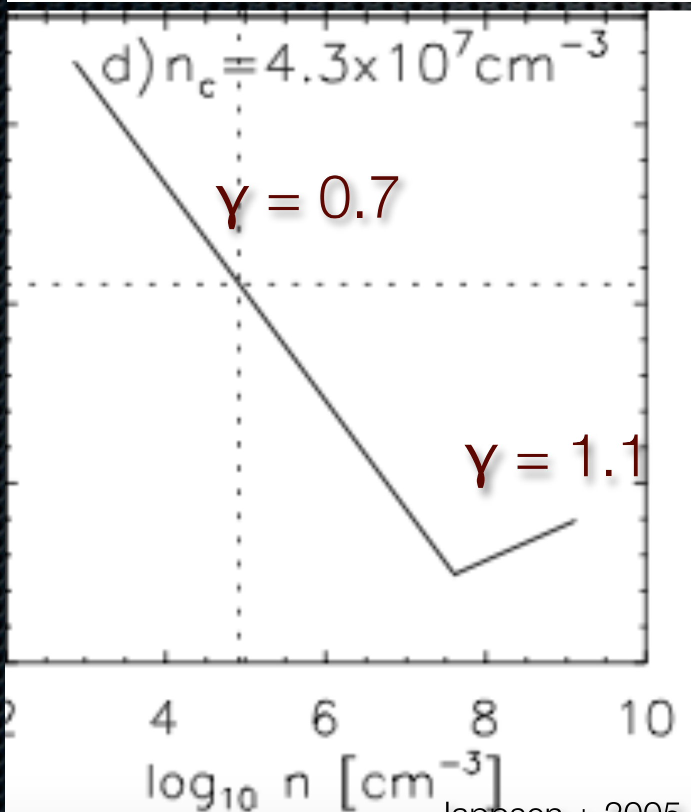

Jappsen + 2005

Cylinders fragment if γ < 1

(Mestel 1965a)

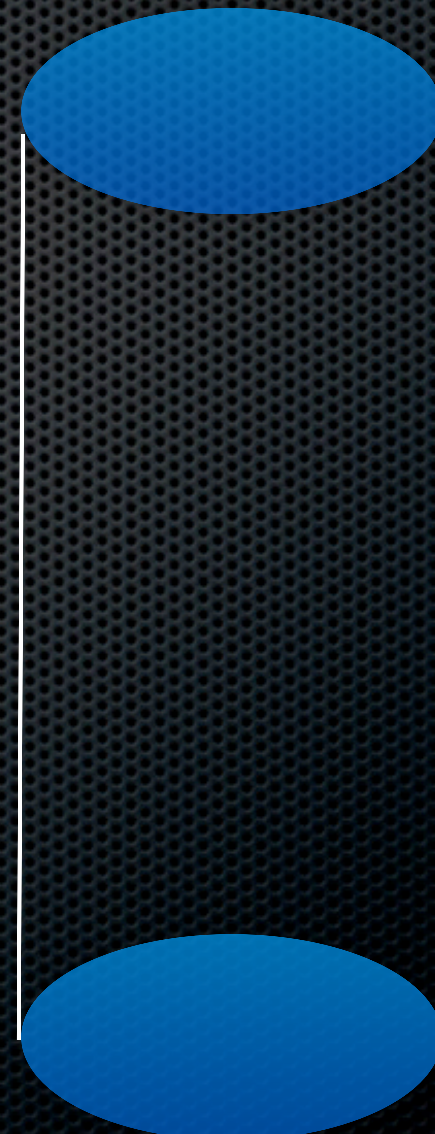

Increasing the transition density to realistic values predicts IMF that agrees with observations

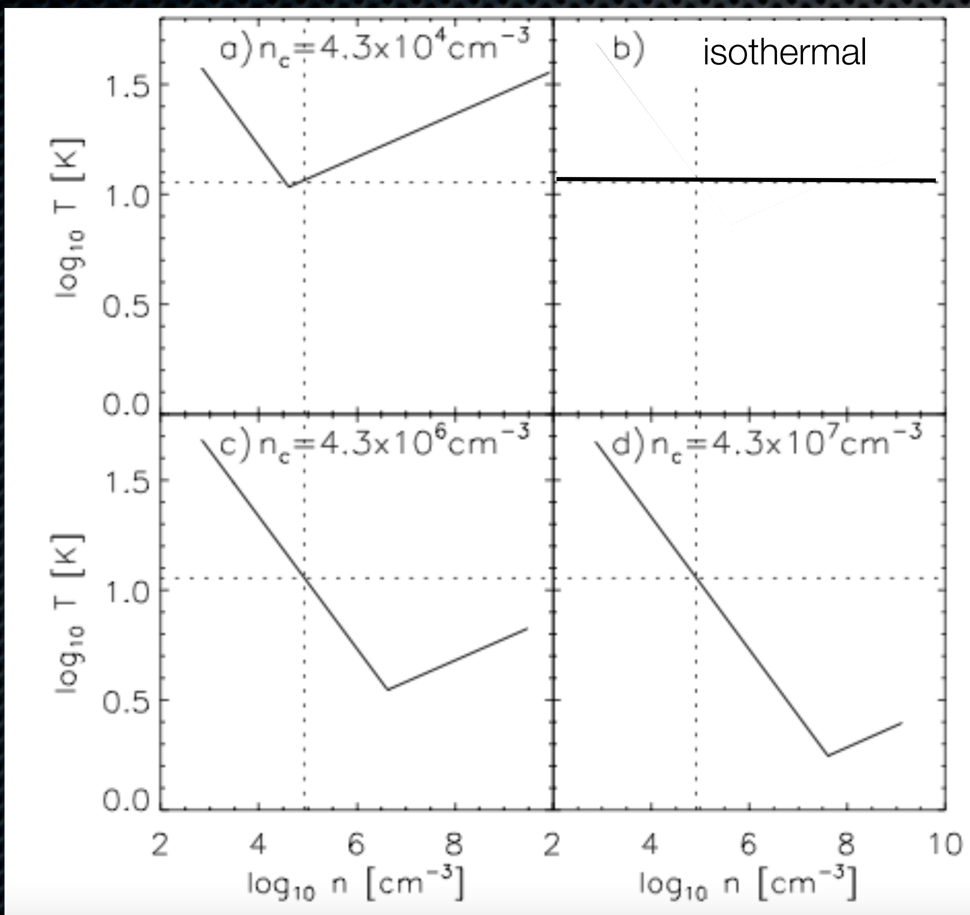

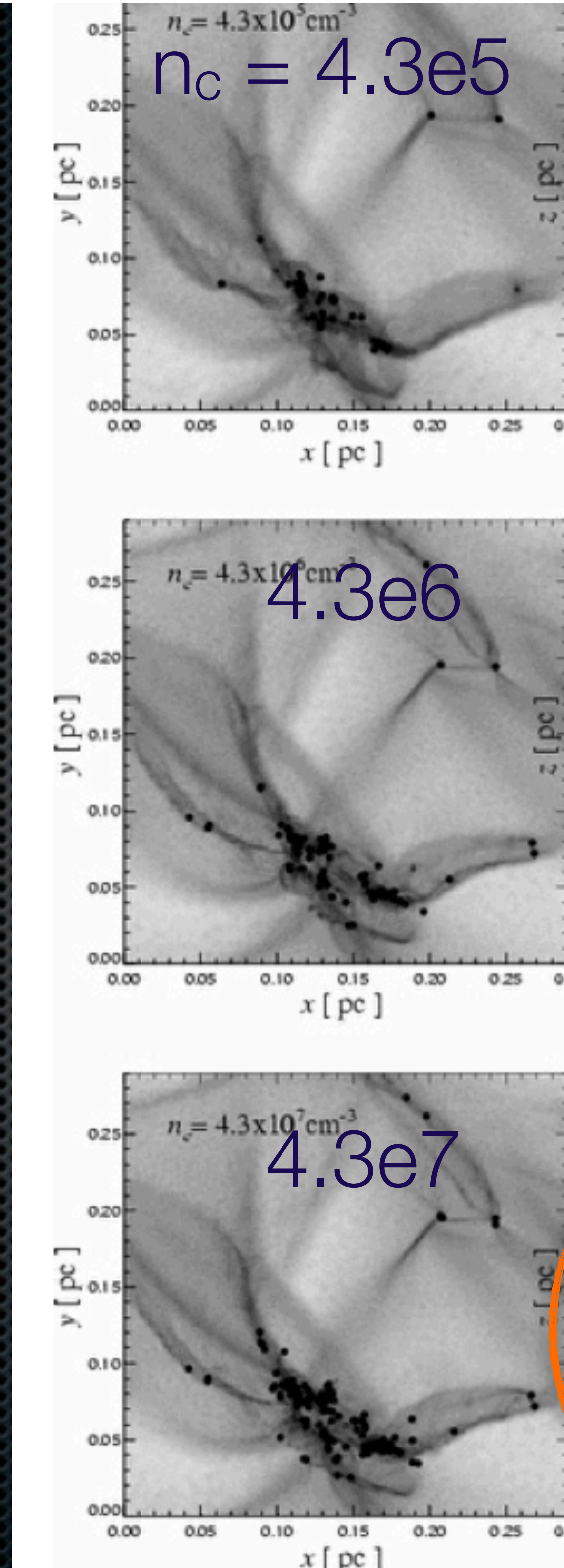

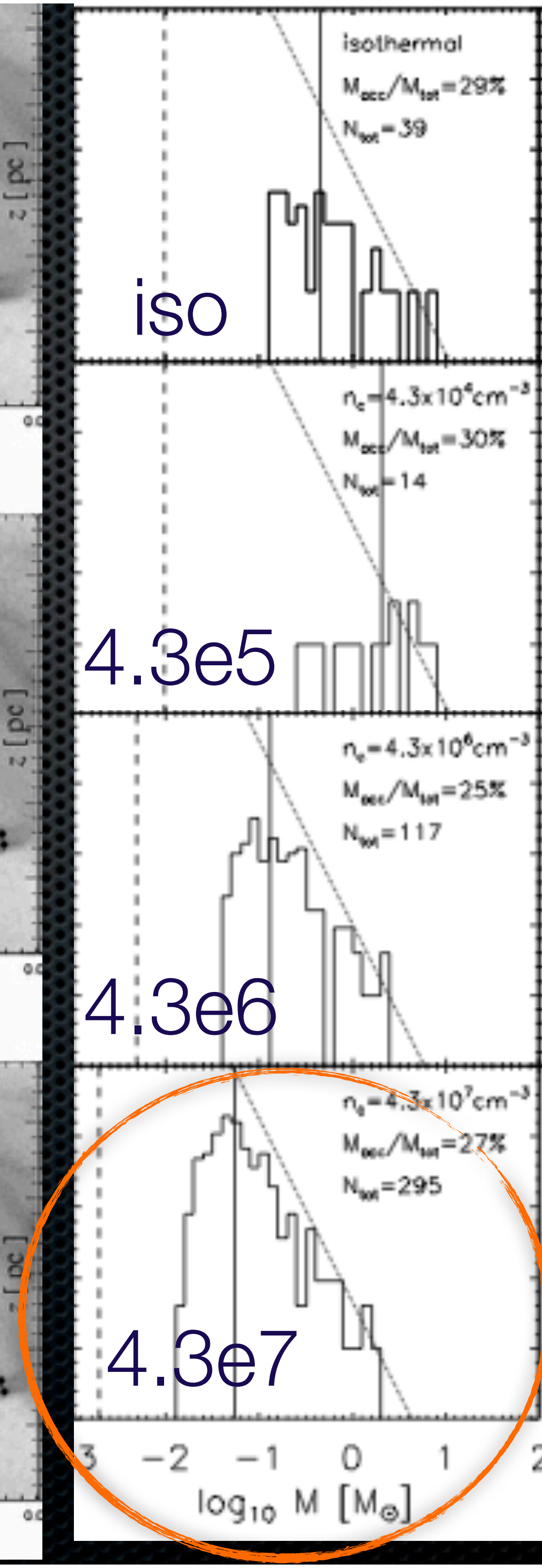

Jappsen, Klessen, Larson, Li, & Mac Low 2005

Turbulent fragmentation also argued to determine IMF

(Padoan 95).

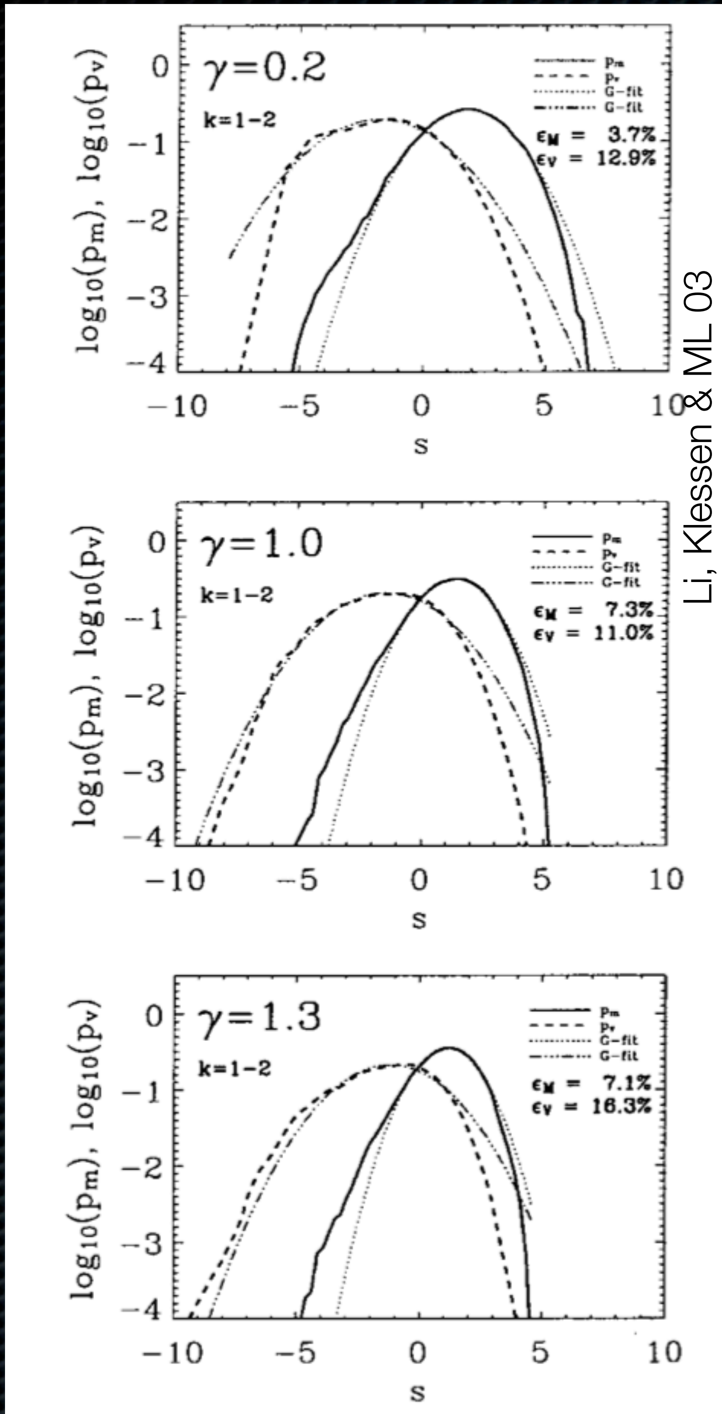

Li, Klessen & ML 03

see Ostriker + 01 for isothermal model

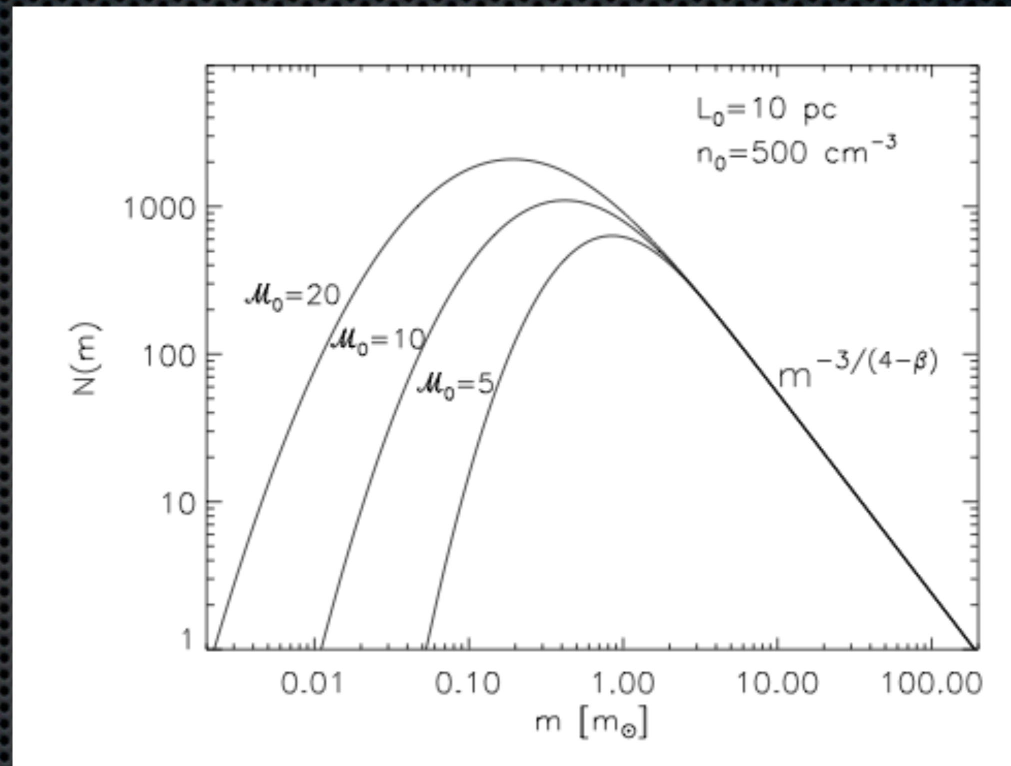

Padoan & Nordlund 02

PDF used to derive fraction of mass in clumps characterized by post-shock density

However, it has become clear that a hierarchical description of collapse is required to capture the behavior of molecular clouds

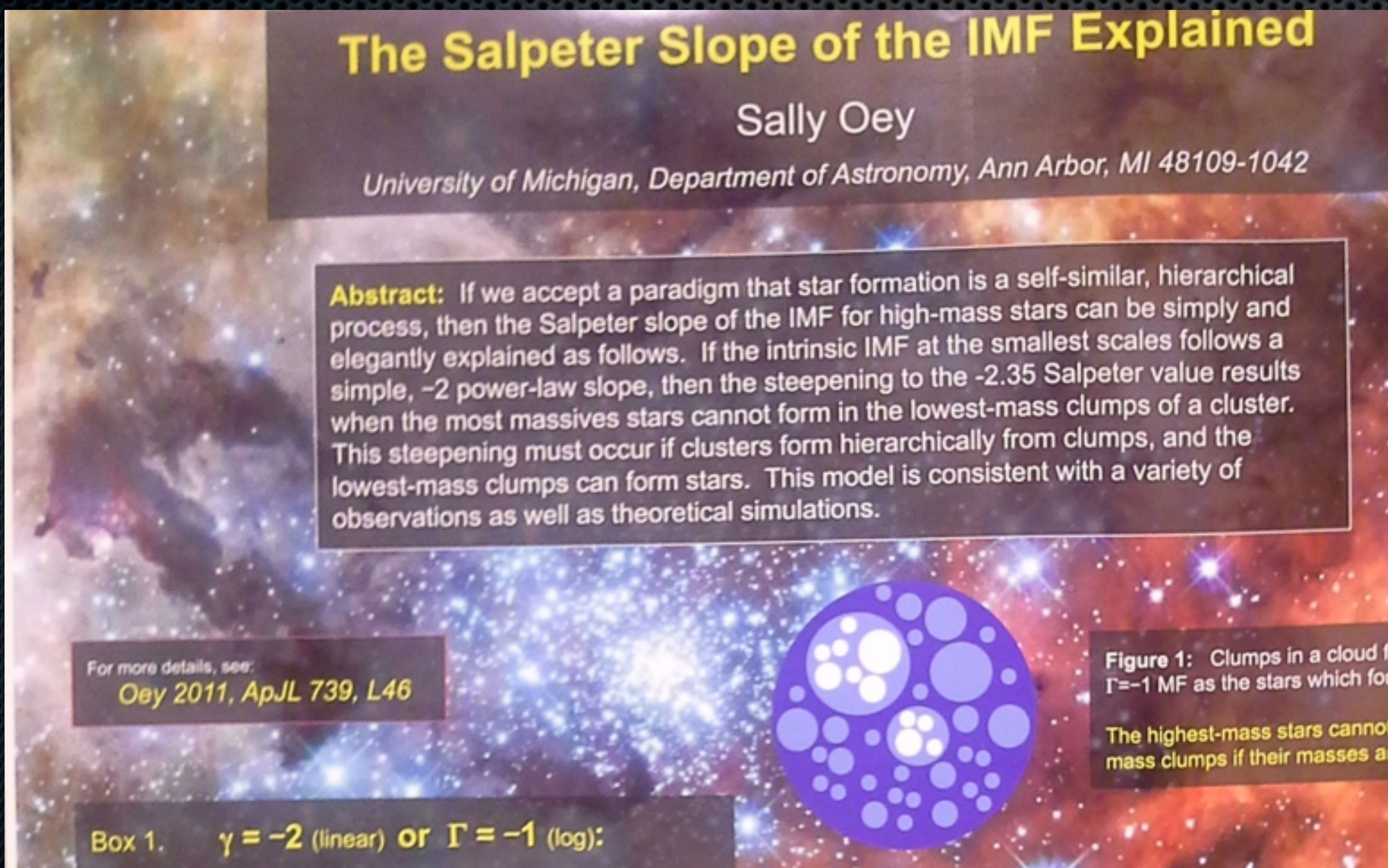

However, it has become clear that a hierarchical description of collapse is required to capture the

Summary. Data for many molecular clouds and condensations show that the internal velocity dispersion of each region is well correlated with its size and mass, and these correlations are approximately of power-law form. The dependence of velocity dispersion on region size is similar to the Kolmogoroff law for subsonic turbulence, suggesting that the observed motions are all part of a common hierarchy of interstellar turbulent motions. The regions studied are mostly gravitationally bound and in approximate virial equilibrium. However, they cannot have formed by simple gravitational collapse, and it appears likely that molecular clouds and their substructures have been created at least partly by processes of supersonic hydrodynamics. The hierarchy of subcondensations may terminate with objects so small that their internal motions are no longer supersonic; this predicts a minimum protostellar mass of the order of a few tenths of a solar mass. Massive 'protostellar'

Larson 81

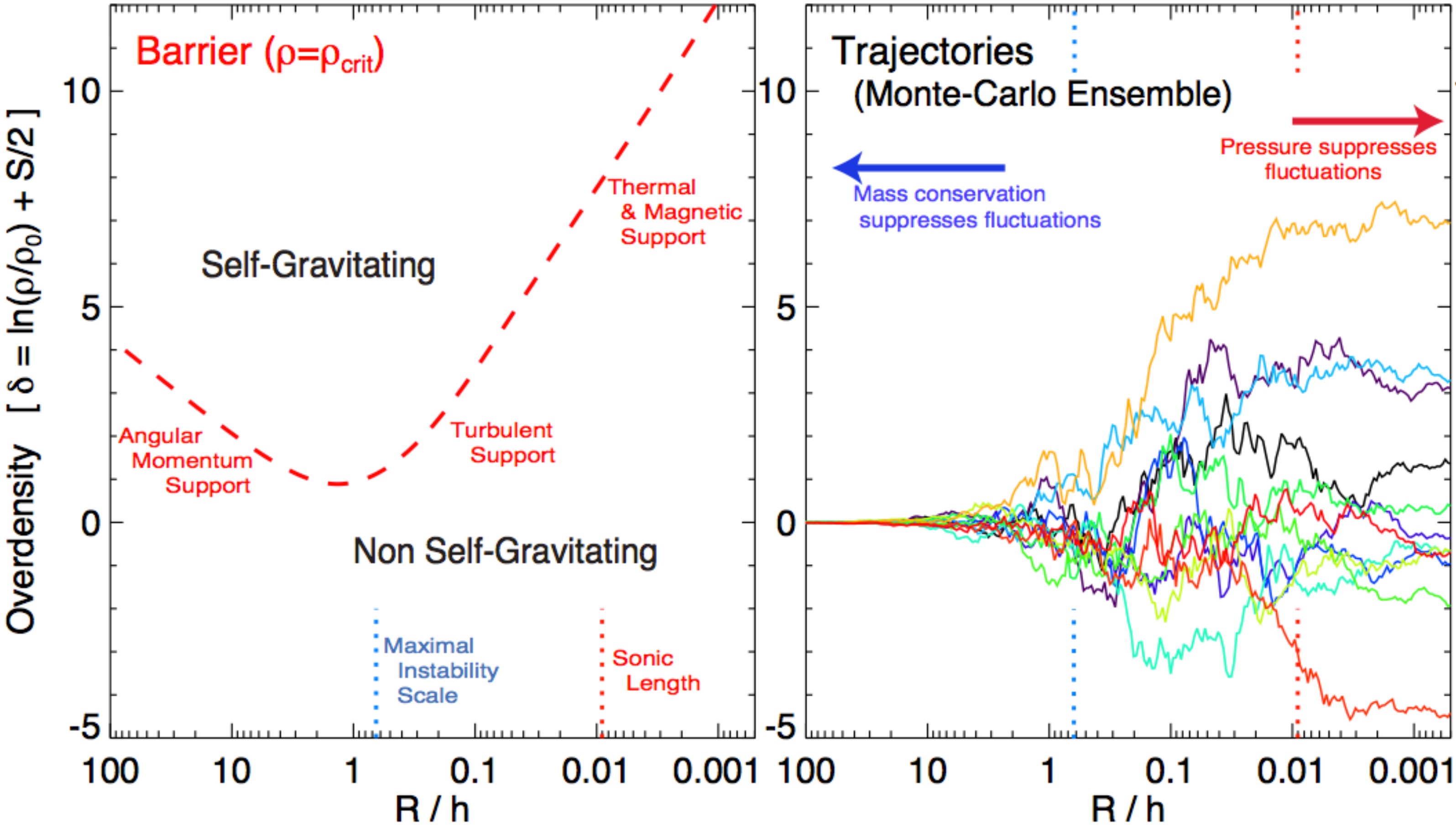

Hopkins 12, ArXiv:1210.0903

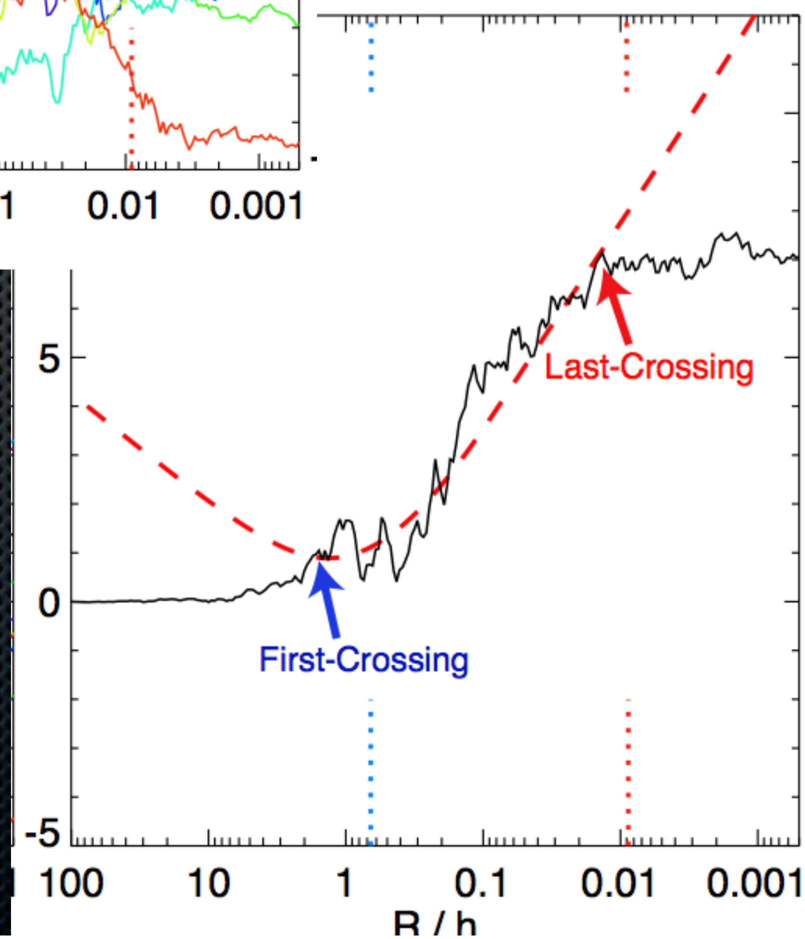

Use full excursion set formalism from Press-Schechter theory to jointly follow hierarchical collapse at all scales simultaneously

Hopkins 12, ArXiv:1210.0903

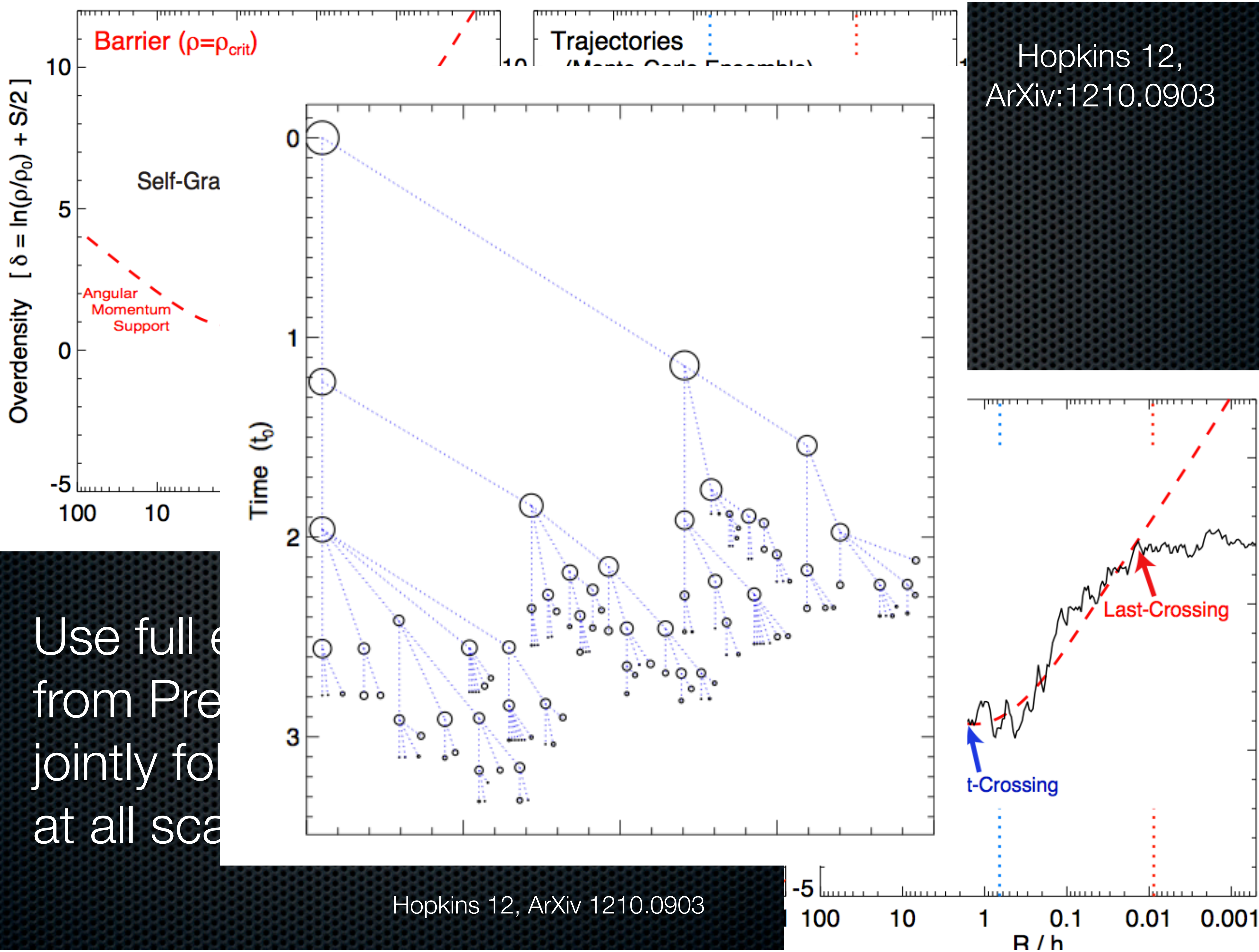

Use full e
from Pre
jointly fo
at all sca

Hopkins 12, ArXiv 1210.0903

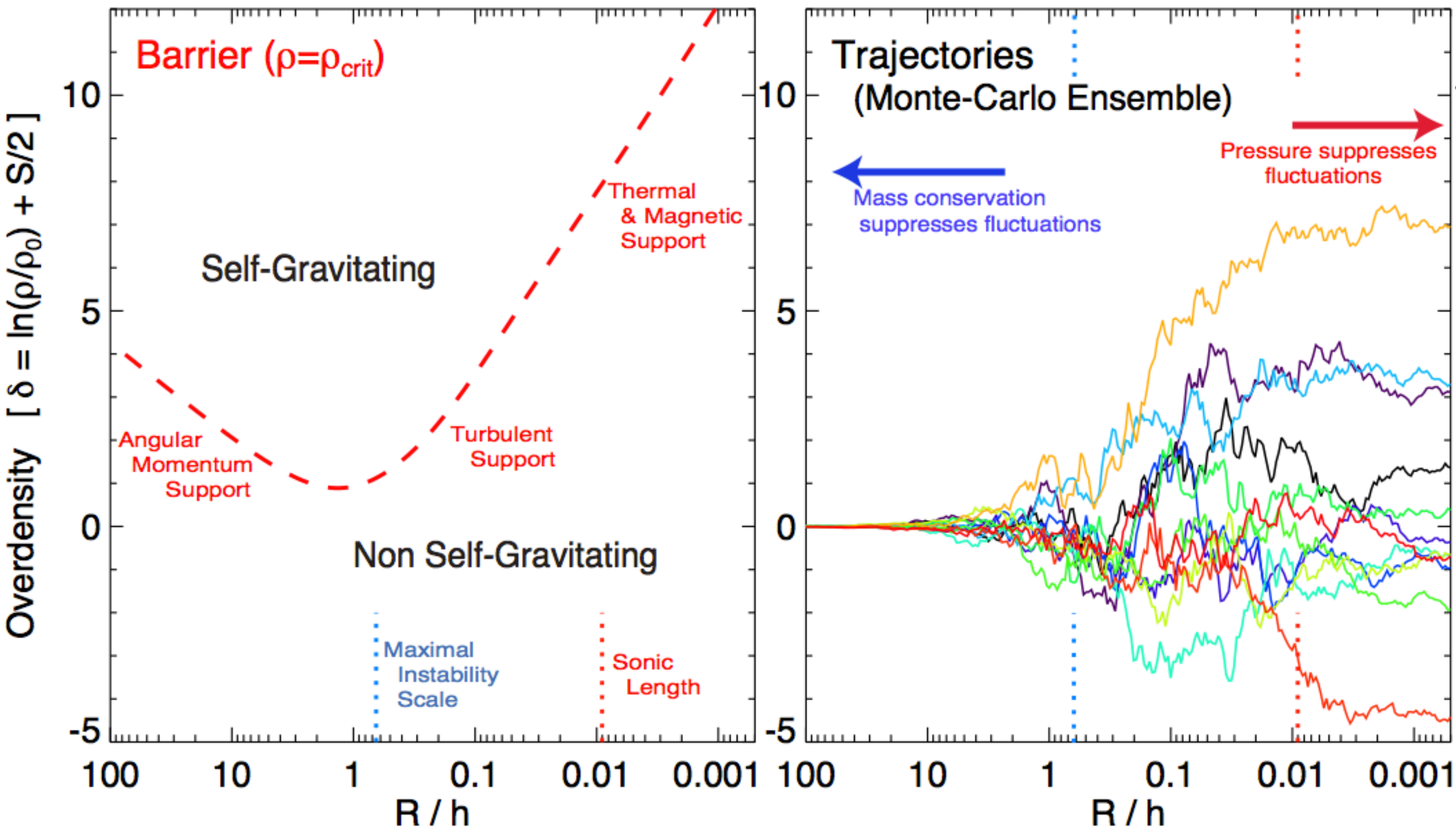

Hopkins 12, ArXiv:1210.0903

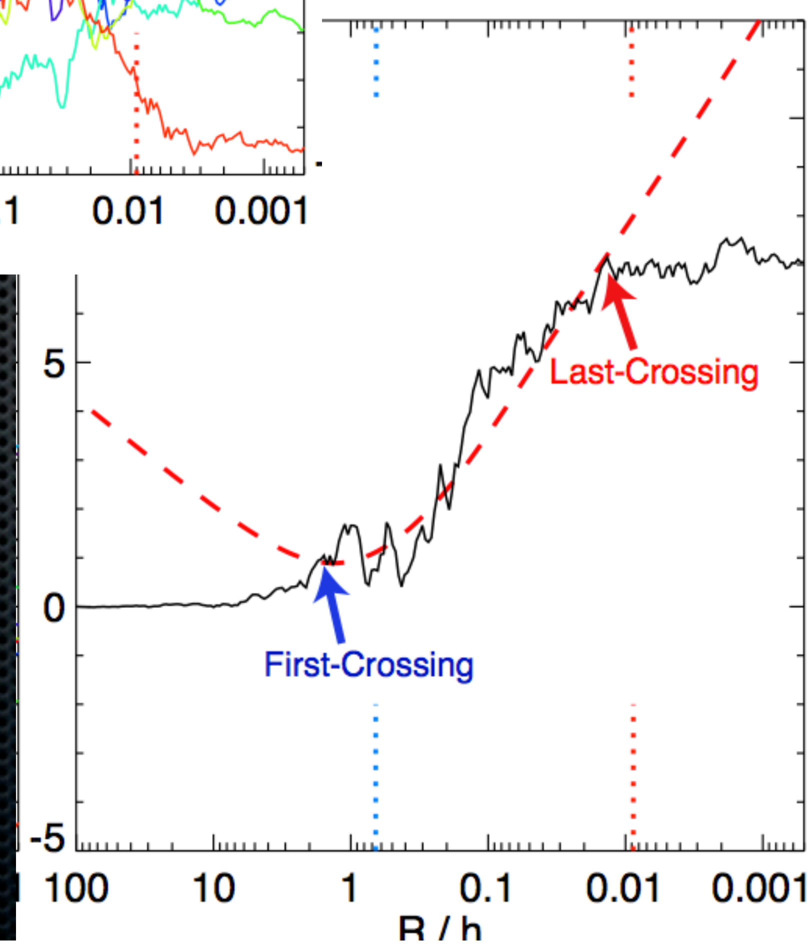

Use full excursion set formalism from Press-Schechter theory to jointly follow hierarchical collapse at all scales simultaneously

Hopkins 12
(MNRAS 423, 2037)

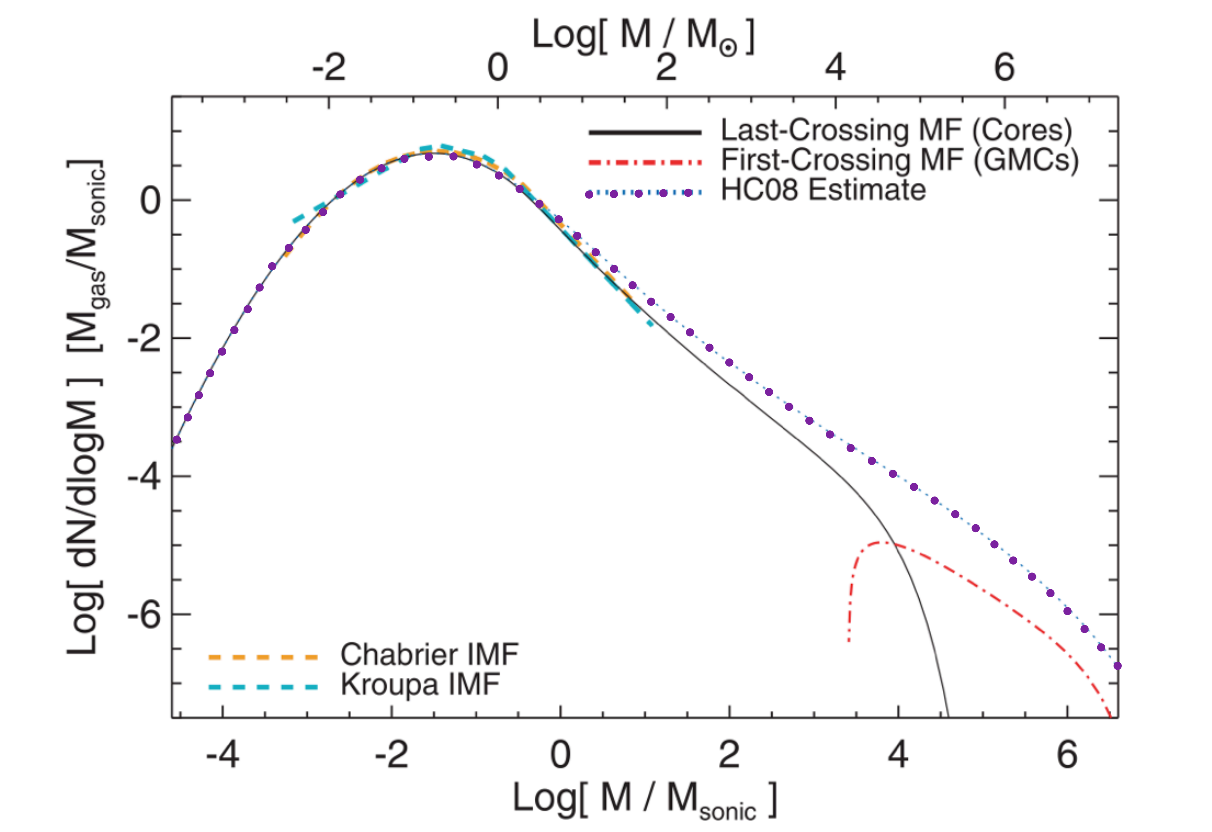

Hennebelle & Chabrier 08 derived mass distribution ignoring multiple barrier crossings.

Hopkins 12 examines first, last crossings as separate distributions.

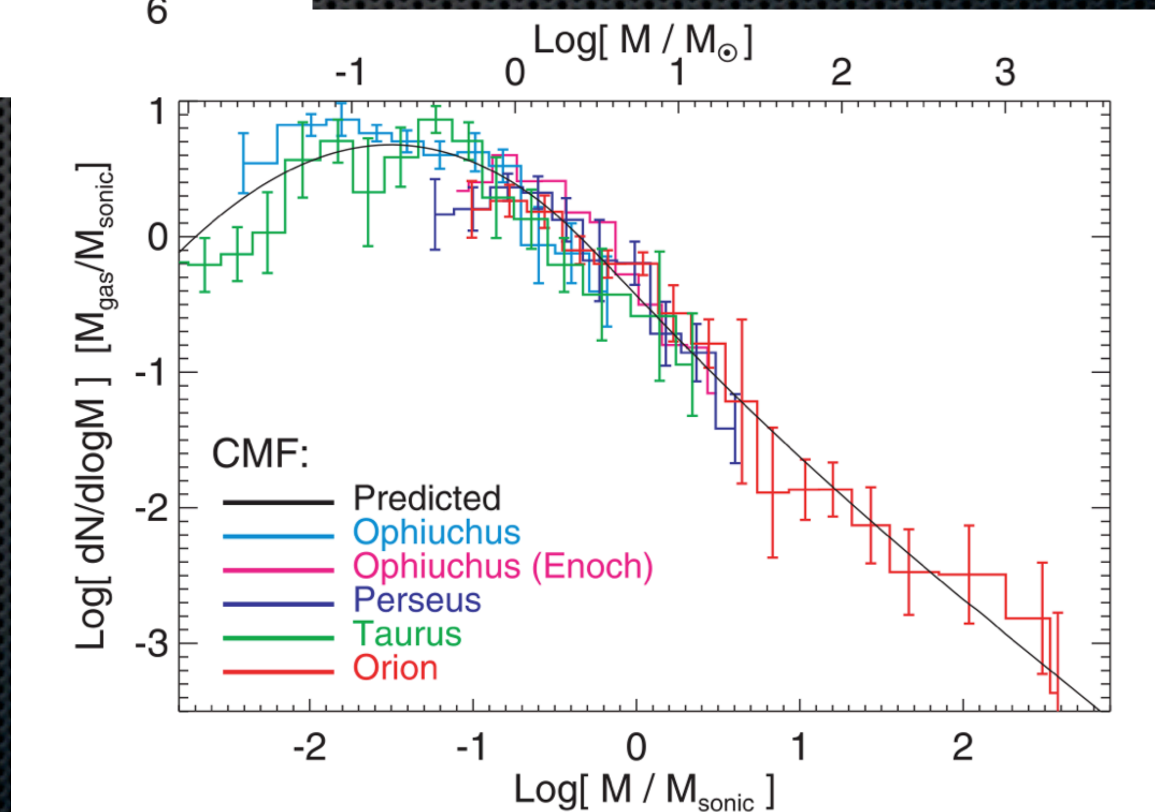

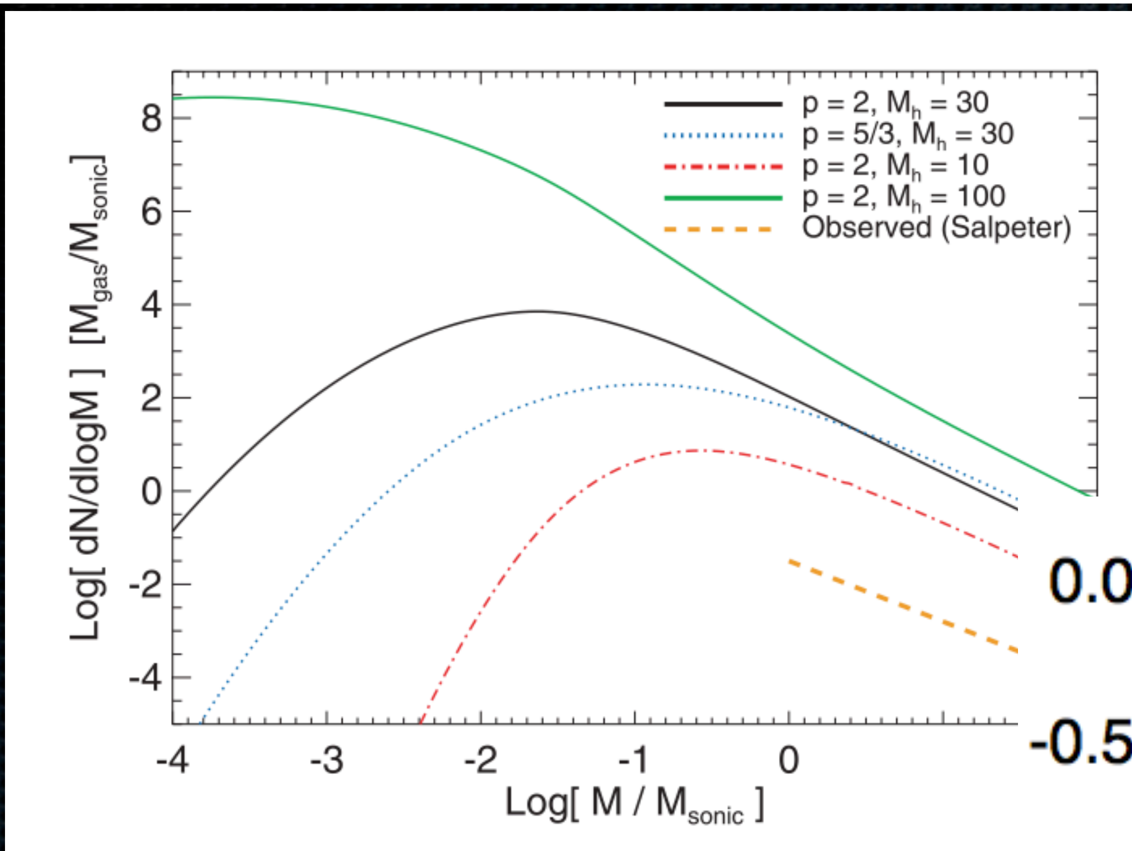

Hopkins 12 (MNRAS 423, 2037)

Hopkins 12, ArXiv 1210.0903

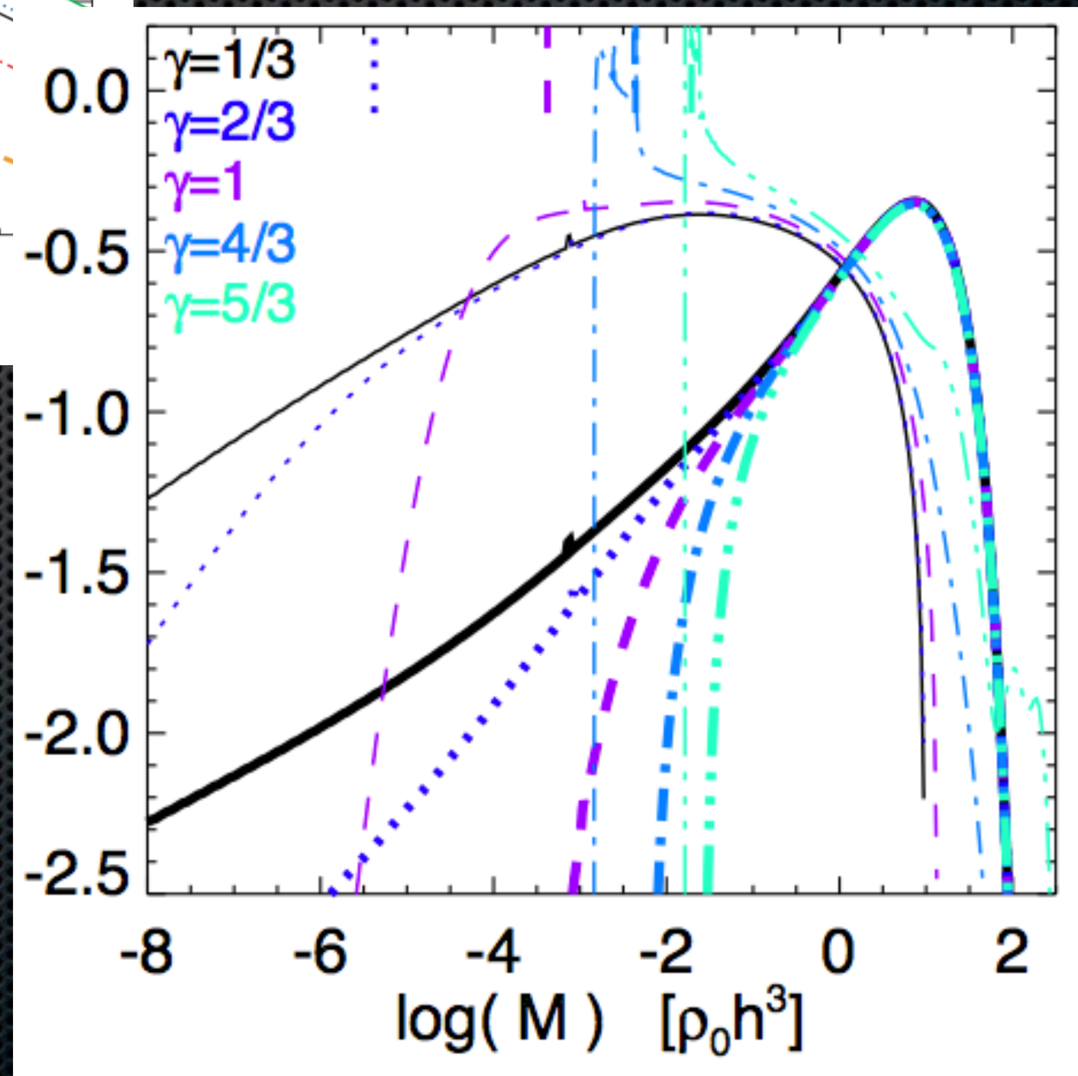

Formalism can be generalized to include non-isothermal EOS, varying turbulent properties, other physics.

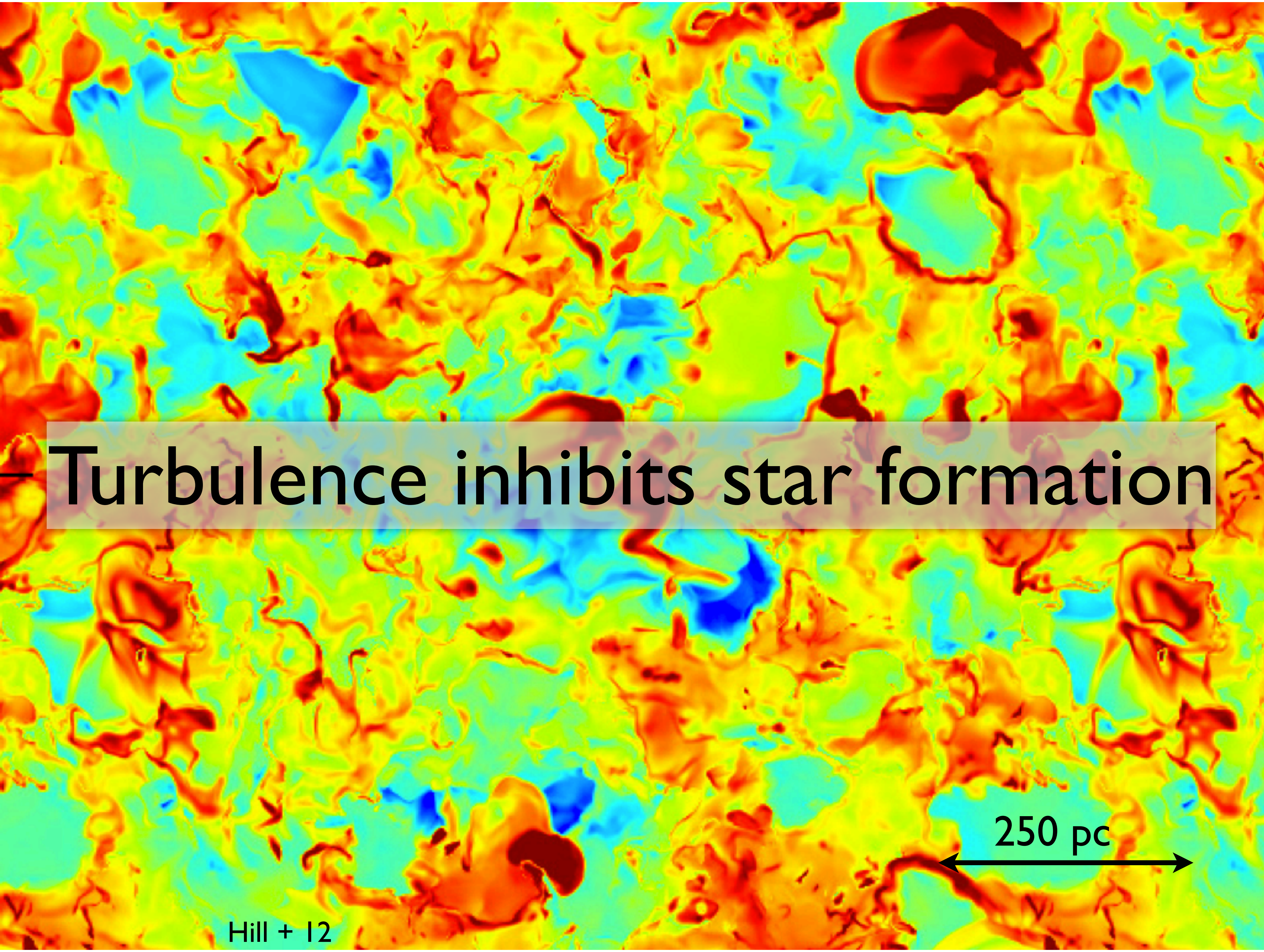
Turbulence inhibits star formation
250 pc
Hill + 12

Turbulence *Prevents* Collapse

- Turbulent motions can be treated as an additional pressure (Chandrasekhar 1951, von Weizsäcker 1951)

$$c_{s,\mathrm{eff}}^2 = c_s^2 + \frac{\langle v^2 \rangle}{3}$$

- Supersonic turbulence increases the mass supported against collapse

$$M_J = \left(\frac{\pi}{G}\right)^{3/2} \rho^{-1/2} \; c_{s,\mathrm{eff}}^3$$

Mac Low & Klessen 04

Turbulence *Promotes* Collapse

- Supersonic turbulence drives shock waves that produce density enhancements.
- In isothermal gas, the postshock density increases with the Mach number M as

$$\rho_s = \rho M^2$$

- Supersonic turbulence decreases the mass supported against collapse

$$M_J = \left(\frac{\pi}{G}\right)^{3/2} \rho_s^{-1/2} c_{s,\mathrm{eff}}^3$$

Mac Low & Klessen 04

Turbulence *Inhibits* Collapse

$$M_J = \left(\frac{\pi}{G}\right)^{3/2} \rho_s^{-1/2} c_{s,\mathrm{eff}}^3 \propto$$

$$\propto \frac{c_s}{v}\left(c_s^2 + \frac{\langle v^2 \rangle}{3}\right)^{3/2} \sim \quad v^2$$

- Turbulence is intermittent, so uniform pressure does not represent it well.
- On average, increasing velocity increases Jeans mass, but locally, compressions can decrease it

Mac Low & Klessen 04

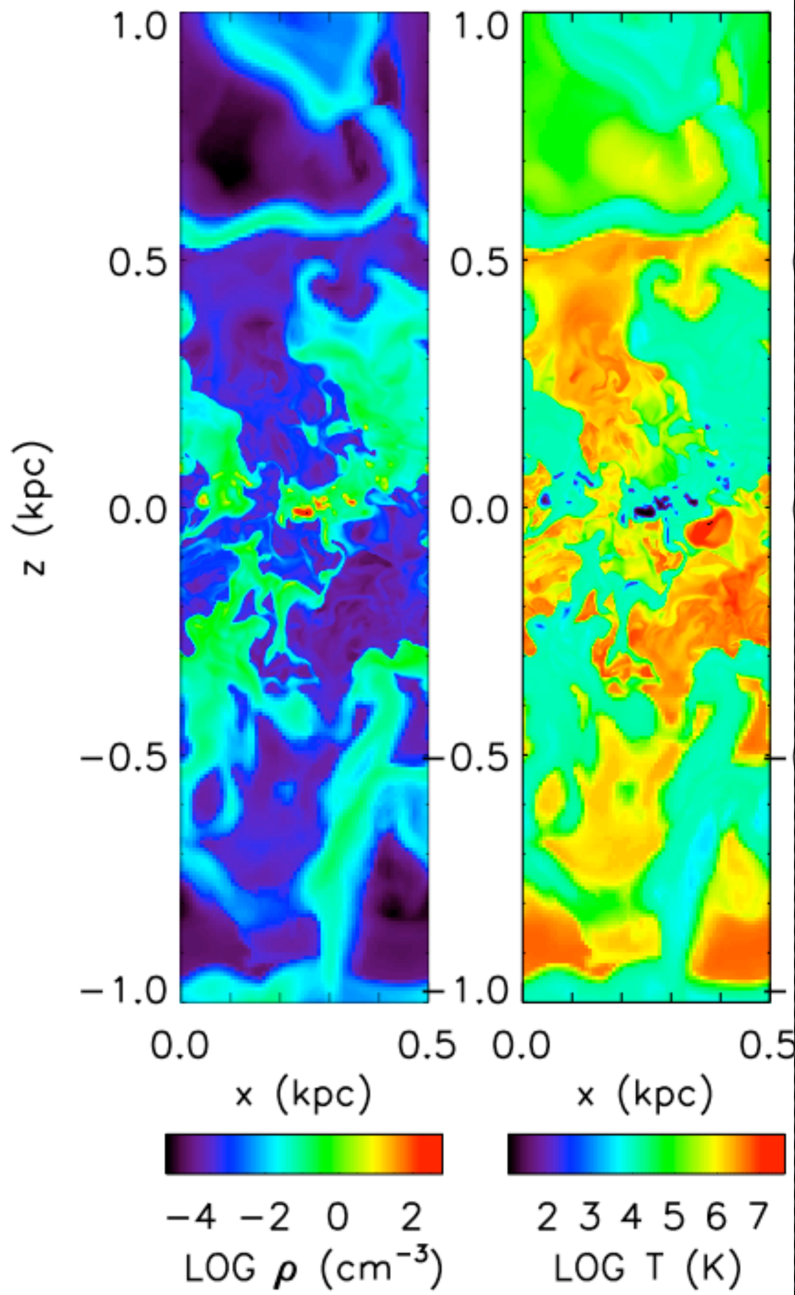

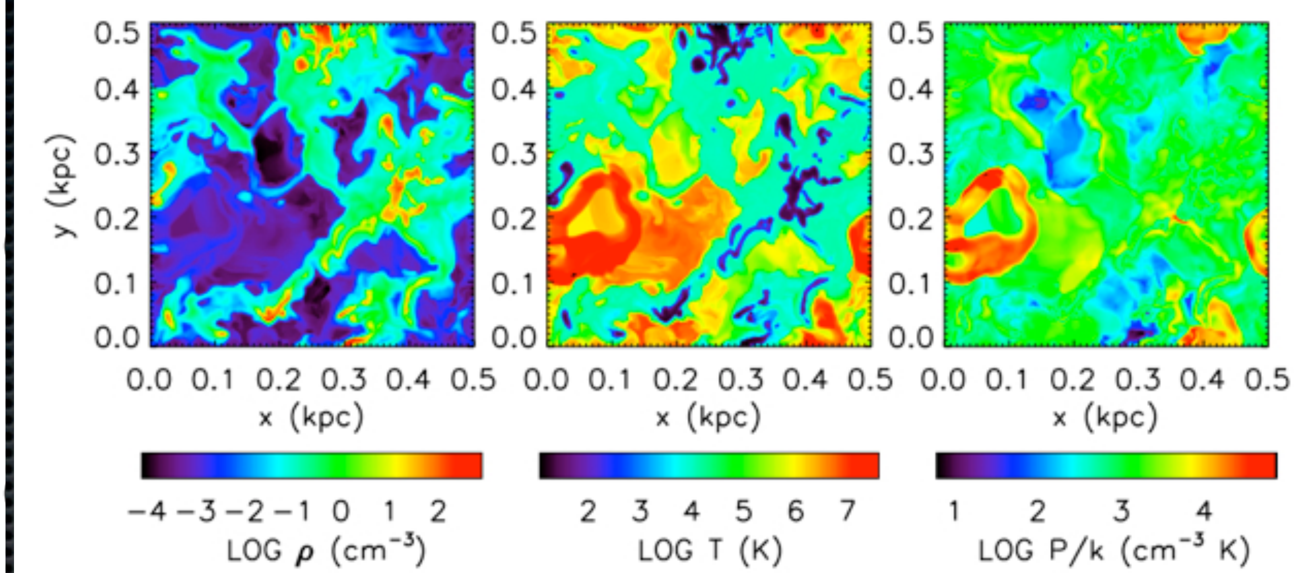

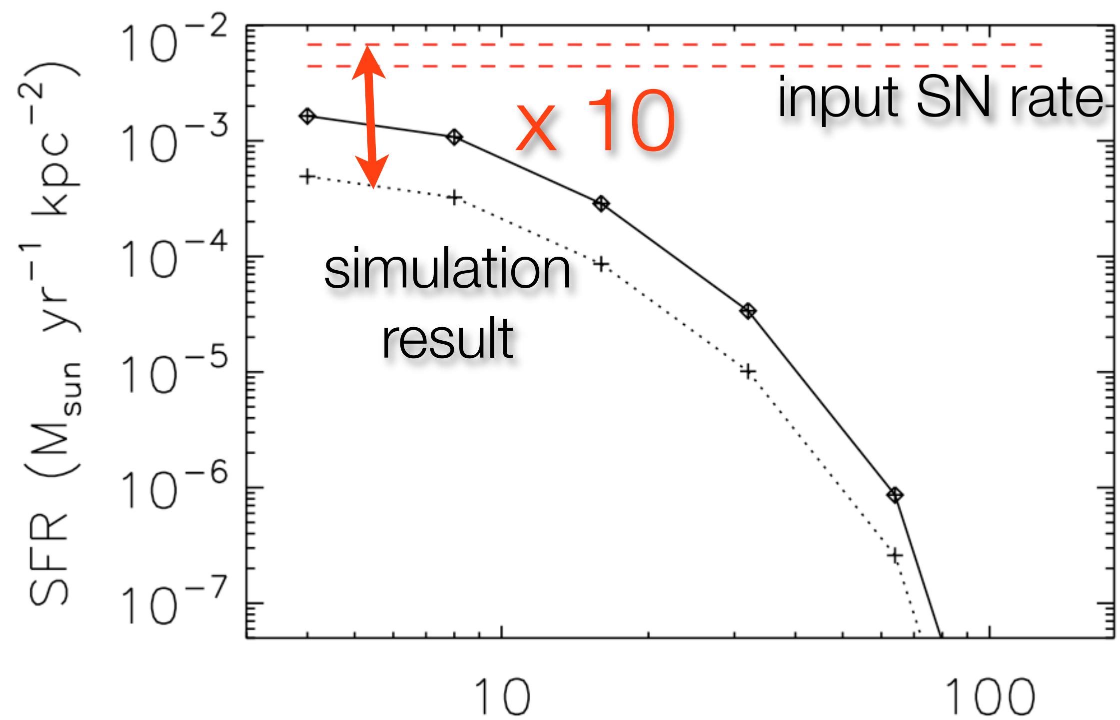

Flash (Fryxell + 00) models of stratified, SN-driven ISM

Joung & Mac Low 2006

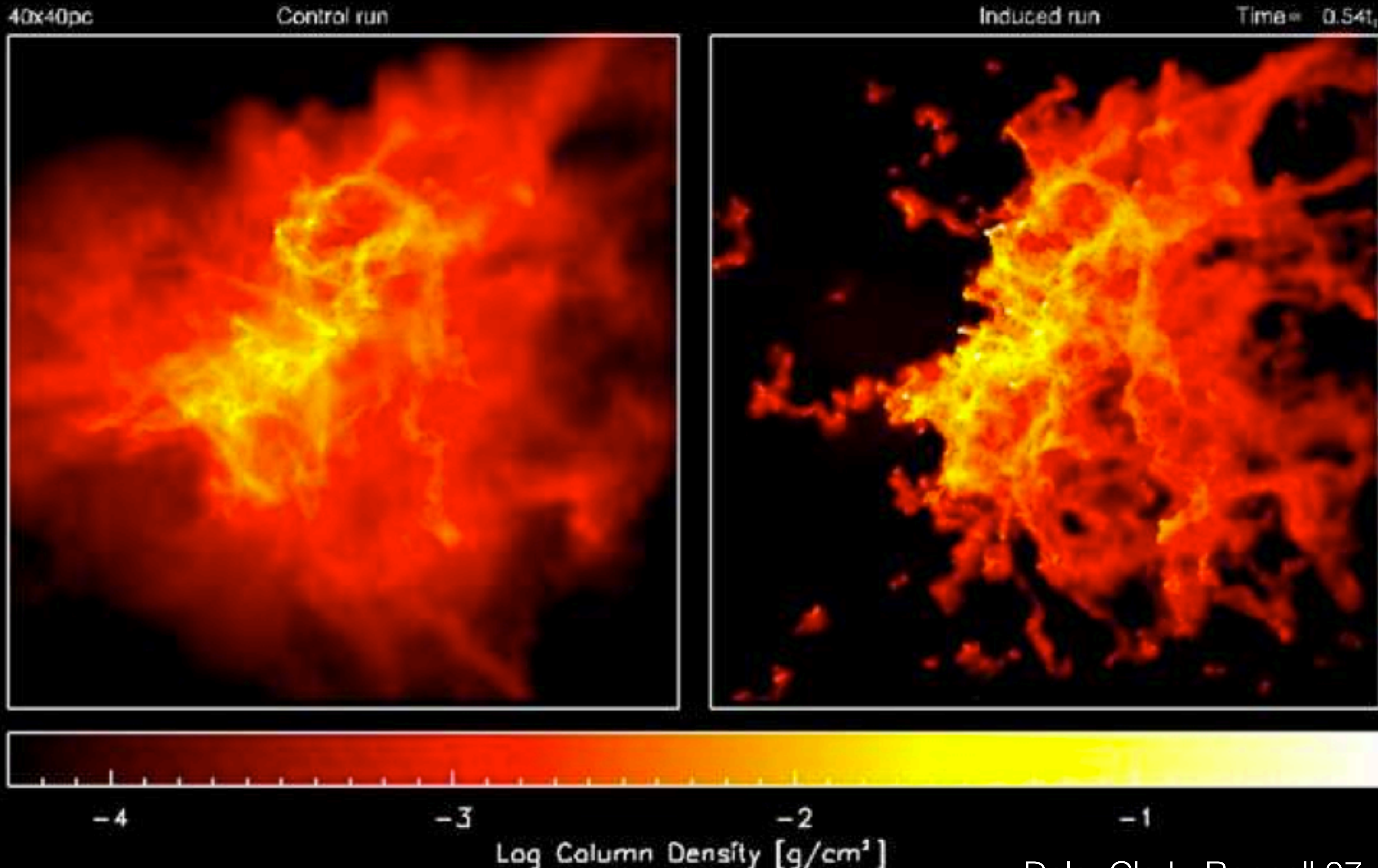

Dale, Clark, Bonnell 07

Star formation sites

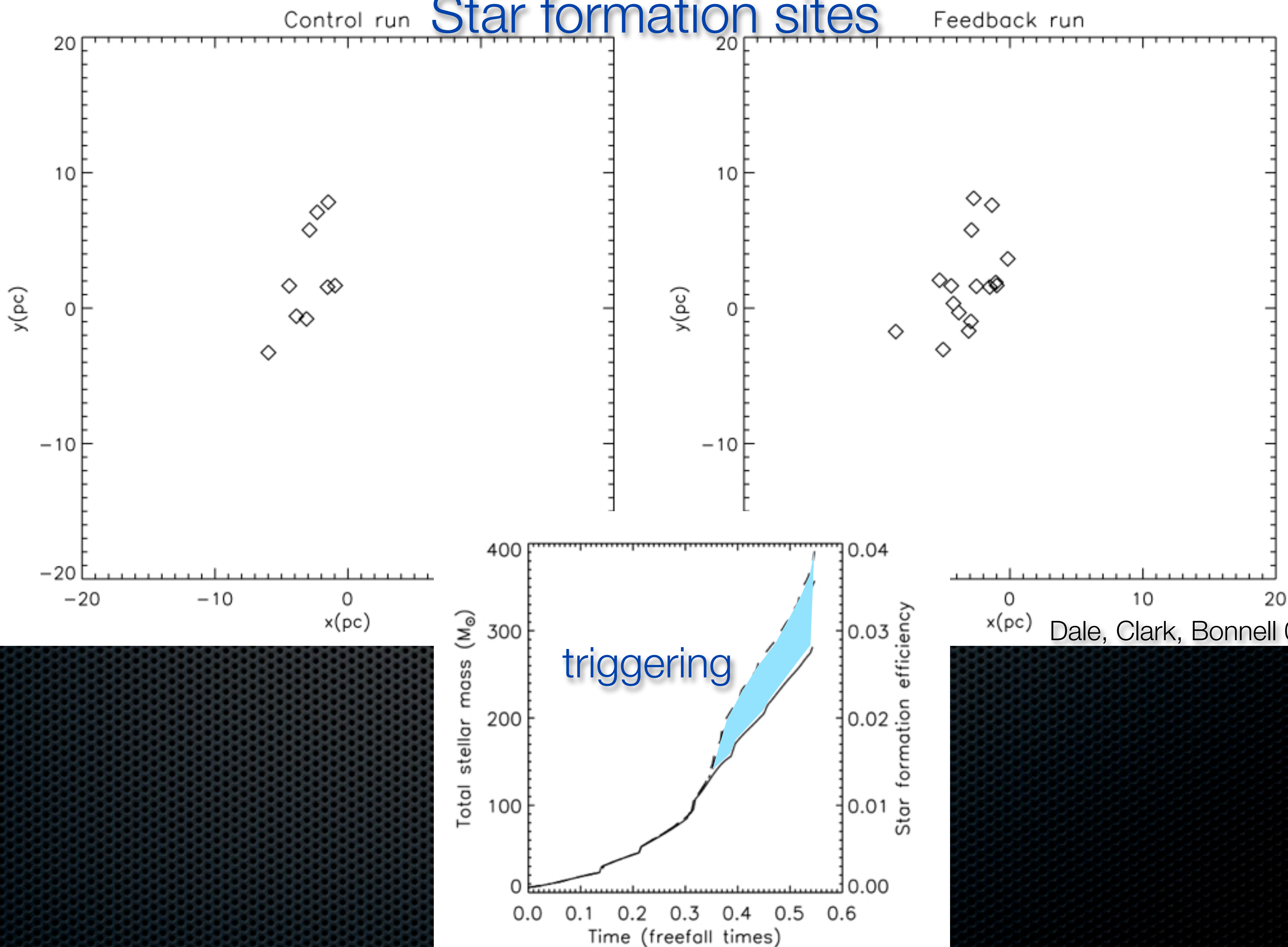

Dale, Clark, Bonnell 07

Quantitative observations of triggering show that most star formation is untriggered

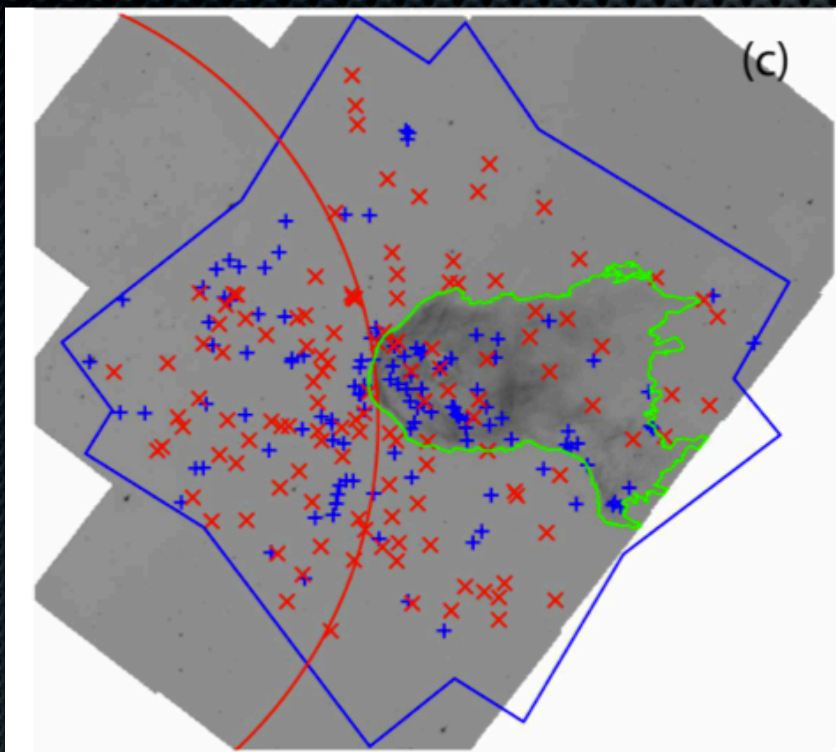

only 14 - 25% of stars in Elephant Trunk Nebula triggered (Getman + 12)

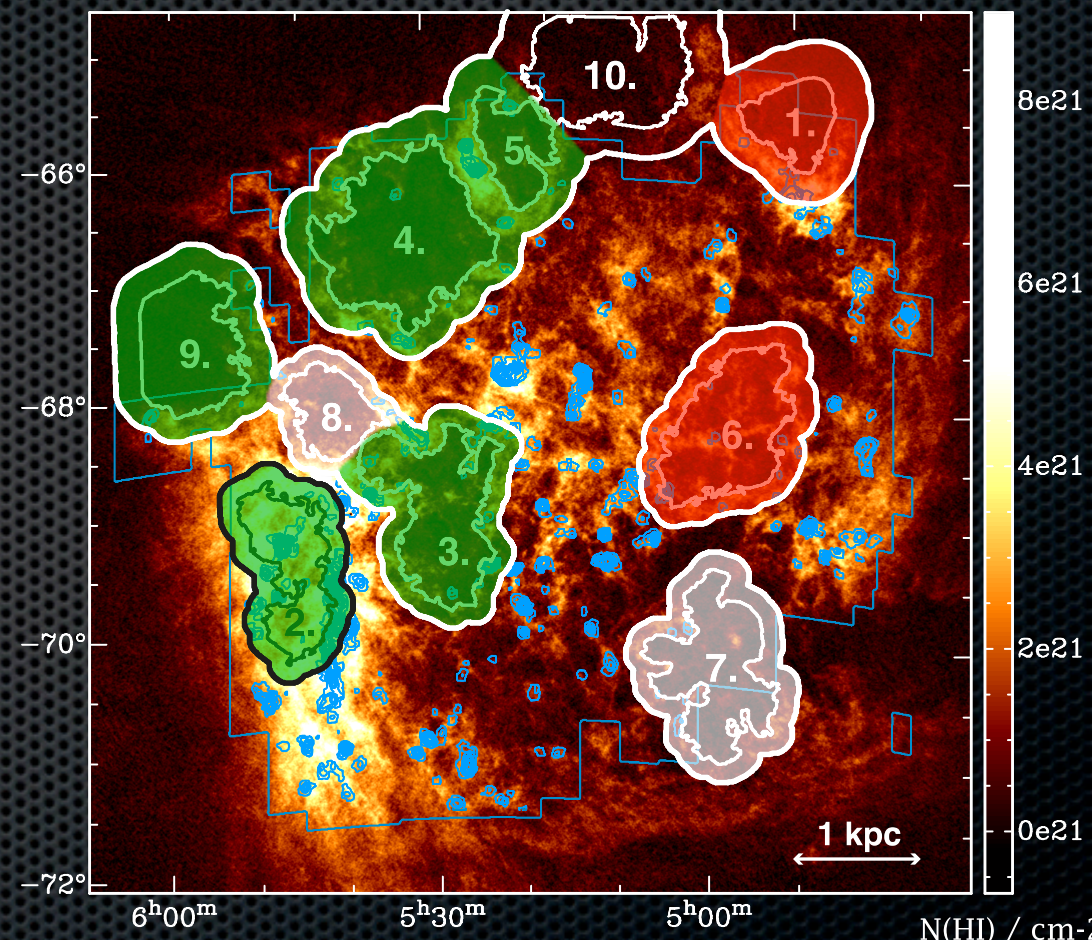

~ 5% of CO in whole LMC formed in shell walls (Dawson + 12)

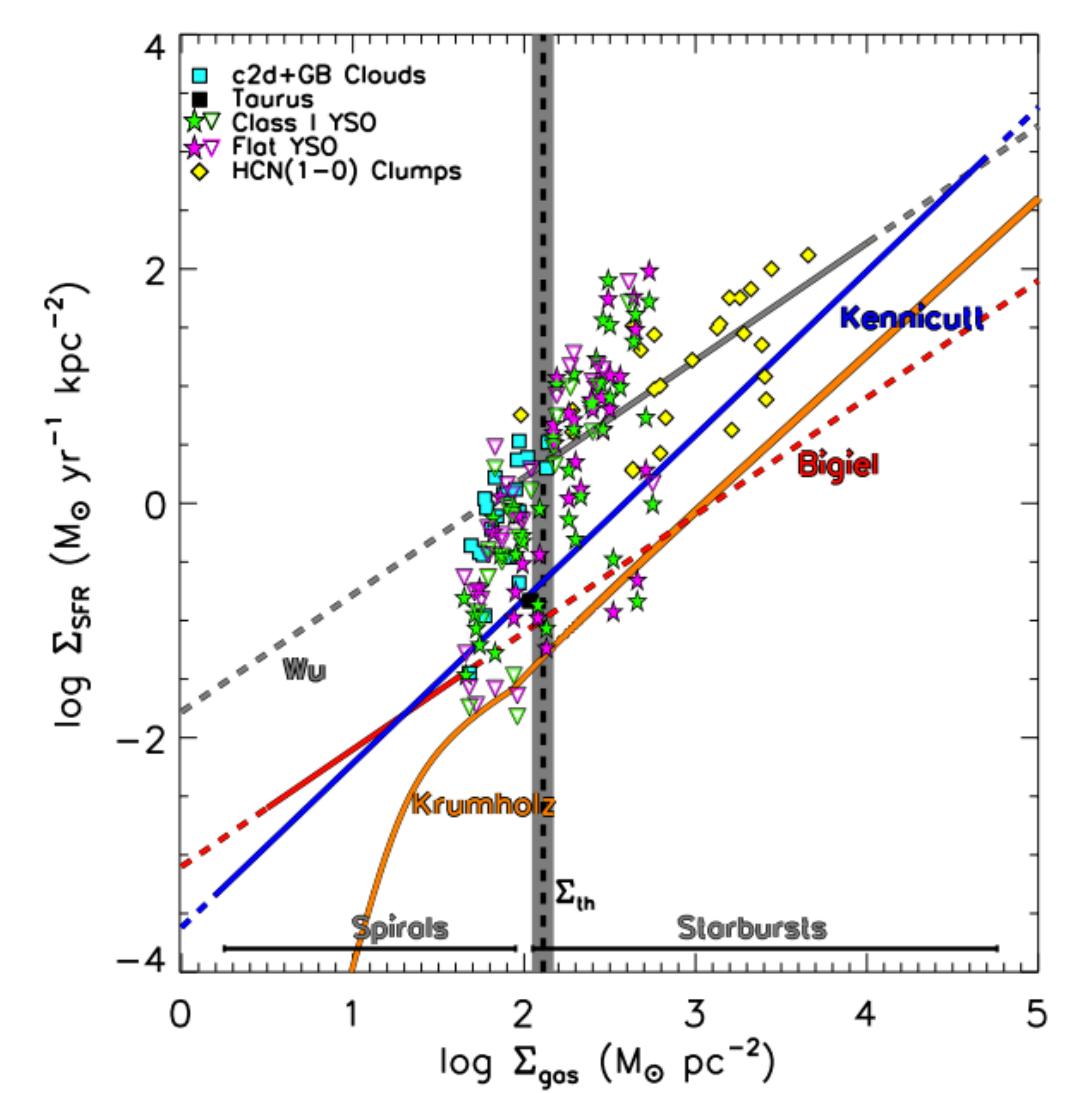

Star Formation Rate

Heiderman + 10

The log-normal density distribution of isothermal turbulence argued to predict the star formation rate.

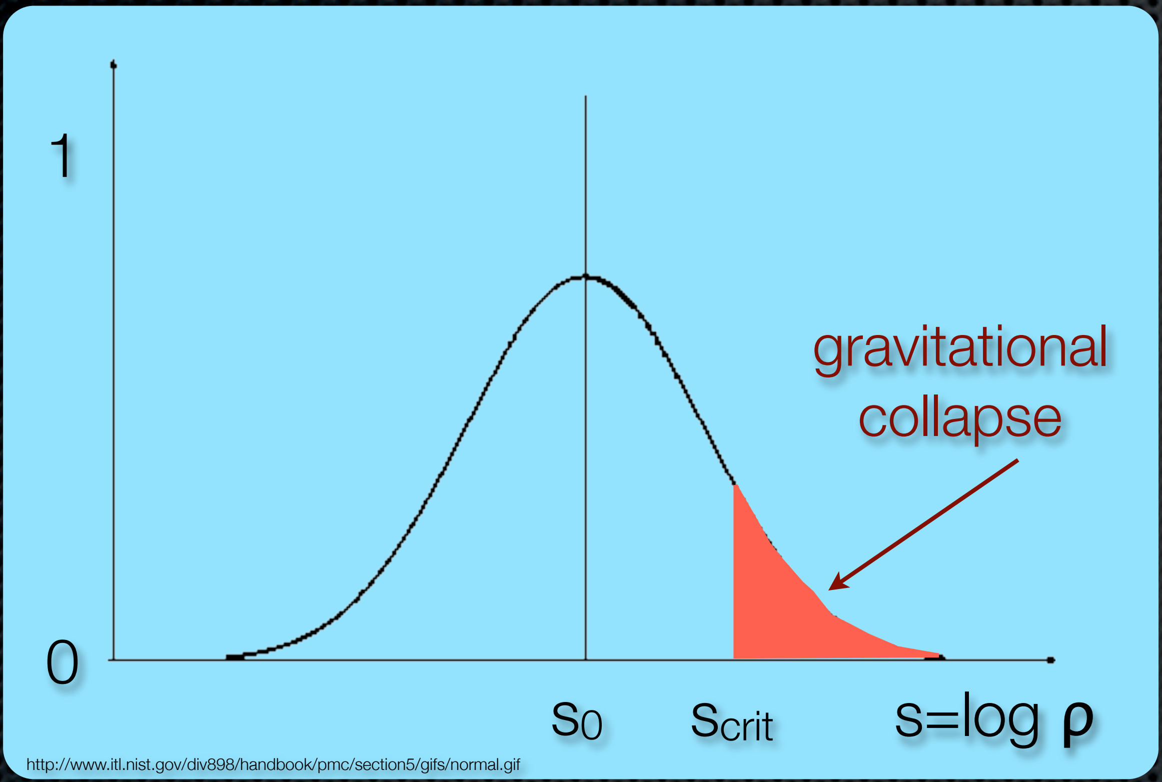

Krumholz & McKee 05
Hennebelle & Chabrier 11
Padoan & Nordlund 11
Padoan + 12
Federrath & Klessen 12

derived from similar arguments for the IMF starting with Padoan 95 and Padoan & Nordlund 02.

Models differ on how to choose the relevant density and free-fall time:

$$\mathrm{SFR} \equiv \frac{M_{\mathrm{c}}}{t_{\mathrm{ff}}(\rho_0)}\,\mathrm{SFR}_{\mathrm{ff}}$$

$$\mathrm{SFR}_{\mathrm{ff}} = \frac{\epsilon}{\phi_t}\int_{s_{\mathrm{crit}}}^{\infty} \frac{t_{\mathrm{ff}}(\rho_0)}{t_{\mathrm{ff}}(\rho)}\,\frac{\rho}{\rho_0}\,p(s)\,\mathrm{d}s$$

Federrath & Klessen 12

Analytic Model	Freefall-time Factor	Critical Density $\rho_{\mathrm{crit}}/\rho_0 = \exp(s_{\mathrm{crit}})$
KM	1	$(\pi^2/5)\,\phi_x^2 \times \alpha_{\mathrm{vir}}\mathcal{M}^2\,(1+\beta^{-1})^{-1}$
PN	$t_{\mathrm{ff}}(\rho_0)/t_{\mathrm{ff}}(\rho_{\mathrm{crit}})$	$(0.067)\,\theta^{-2}\times \alpha_{\mathrm{vir}}\mathcal{M}^2 f(\beta)$
HC	$t_{\mathrm{ff}}(\rho_0)/t_{\mathrm{ff}}(\rho)$	$(\pi^2/5)\,y_{\mathrm{cut}}^{-2}\times \alpha_{\mathrm{vir}}\mathcal{M}^{-2}\,(1+\beta^{-1}) + \tilde{\rho}_{\mathrm{crit,turb}}$
multi-ff KM	$t_{\mathrm{ff}}(\rho_0)/t_{\mathrm{ff}}(\rho)$	$(\pi^2/5)\,\phi_x^2 \times \alpha_{\mathrm{vir}}\mathcal{M}^2\,(1+\beta^{-1})^{-1}$
multi-ff PN	$t_{\mathrm{ff}}(\rho_0)/t_{\mathrm{ff}}(\rho)$	$(0.067)\,\theta^{-2}\times \alpha_{\mathrm{vir}}\mathcal{M}^2 f(\beta)$
multi-ff HC	$t_{\mathrm{ff}}(\rho_0)/t_{\mathrm{ff}}(\rho)$	$(\pi^2/5)\,y_{\mathrm{cut}}^{-2}\times \alpha_{\mathrm{vir}}\mathcal{M}^{-2}\,(1+\beta^{-1})$

original
(Krumholz & McKee 05)

magnetic fields
(Padoan & Nordlund 11)

multi-density
(Hennebelle & Chabrier 11)

combined
(Federrath & Klessen 12)

Models differ on how to choose the relevant density and free-fall time:

$$\mathrm{SFR} \equiv \frac{M_c}{t_{\mathrm{ff}}(\rho_0)}\,\mathrm{SFR}_{\mathrm{ff}}$$

$$\mathrm{SFR}_{\mathrm{ff}} = \frac{\epsilon}{\phi_t}\int_{s_{\mathrm{crit}}}^{\infty} \frac{t_{\mathrm{ff}}(\rho_0)}{t_{\mathrm{ff}}(\rho)}\,\frac{\rho}{\rho_0}\,p(s)\,\mathrm{d}s$$

Federrath & Klessen 12

Analytic Model	Freefall-time Factor	Critical Density $\rho_{\mathrm{crit}}/\rho_0 = \exp(s_{\mathrm{crit}})$
KM	1	$(\pi^2/5)\,\phi_x^2 \times \alpha_{\mathrm{vir}}\mathcal{M}^2\,(1+\beta^{-1})^{-1}$
PN	$t_{\mathrm{ff}}(\rho_0)/t_{\mathrm{ff}}(\rho_{\mathrm{crit}})$	$(0.067)\,\theta^{-2} \times \alpha_{\mathrm{vir}}\mathcal{M}^2 f(\beta)$
HC	$t_{\mathrm{ff}}(\rho_0)/t_{\mathrm{ff}}(\rho)$	$(\pi^2/5)\,y_{\mathrm{cut}}^{-2} \times \alpha_{\mathrm{vir}}\mathcal{M}^{-2}\,(1+\beta^{-1}) + \tilde{\rho}_{\mathrm{crit,turb}}$
multi-ff KM	$t_{\mathrm{ff}}(\rho_0)/t_{\mathrm{ff}}(\rho)$	$(\pi^2/5)\,\phi_x^2 \times \alpha_{\mathrm{vir}}\mathcal{M}^2\,(1+\beta^{-1})^{-1}$
multi-ff PN	$t_{\mathrm{ff}}(\rho_0)/t_{\mathrm{ff}}(\rho)$	$(0.067)\,\theta^{-2} \times \alpha_{\mathrm{vir}}\mathcal{M}^2 f(\beta)$
multi-ff HC	$t_{\mathrm{ff}}(\rho_0)/t_{\mathrm{ff}}(\rho)$	$(\pi^2/5)\,y_{\mathrm{cut}}^{-2} \times \alpha_{\mathrm{vir}}\mathcal{M}^{-2}\,(1+\beta^{-1})$

original
(Krumholz & McKee 05)

magnetic fields
(Padoan & Nordlund 11)

multi-density
(Hennebelle & Chabrier 11)

combined
(Federrath & Klessen 12)

Models differ on how to choose the relevant density and free-fall time:

$$\mathrm{SFR} \equiv \frac{M_c}{t_{\mathrm{ff}}(\rho_0)} \mathrm{SFR}_{\mathrm{ff}}$$

$$\mathrm{SFR}_{\mathrm{ff}} = \frac{\epsilon}{\phi_t} \int_{s_{\mathrm{crit}}}^{\infty} \frac{t_{\mathrm{ff}}(\rho_0)}{t_{\mathrm{ff}}(\rho)} \frac{\rho}{\rho_0} p(s)\, \mathrm{d}s$$

Federrath & Klessen 12

Analytic Model	Freefall-time Factor	Critical Density $\rho_{\mathrm{crit}}/\rho_0 = \exp(s_{\mathrm{crit}})$
KM	1	$(\pi^2/5)\,\phi_x^2 \times \alpha_{\mathrm{vir}}\mathcal{M}^2\,(1+\beta^{-1})^{-1}$
PN	$t_{\mathrm{ff}}(\rho_0)/t_{\mathrm{ff}}(\rho_{\mathrm{crit}})$	$(0.067)\,\theta^{-2} \times \alpha_{\mathrm{vir}}\mathcal{M}^2 f(\beta)$
HC	$t_{\mathrm{ff}}(\rho_0)/t_{\mathrm{ff}}(\rho)$	$(\pi^2/5)\,y_{\mathrm{cut}}^{-2} \times \alpha_{\mathrm{vir}}\mathcal{M}^{-2}\,(1+\beta^{-1}) + \tilde{\rho}_{\mathrm{crit,turb}}$
multi-ff KM	$t_{\mathrm{ff}}(\rho_0)/t_{\mathrm{ff}}(\rho)$	$(\pi^2/5)\,\phi_x^2 \times \alpha_{\mathrm{vir}}\mathcal{M}^2\,(1+\beta^{-1})^{-1}$
multi-ff PN	$t_{\mathrm{ff}}(\rho_0)/t_{\mathrm{ff}}(\rho)$	$(0.067)\,\theta^{-2} \times \alpha_{\mathrm{vir}}\mathcal{M}^2 f(\beta)$
multi-ff HC	$t_{\mathrm{ff}}(\rho_0)/t_{\mathrm{ff}}(\rho)$	$(\pi^2/5)\,y_{\mathrm{cut}}^{-2} \times \alpha_{\mathrm{vir}}\mathcal{M}^{-2}\,(1+\beta^{-1})$

original
(Krumholz & McKee 05)

magnetic fields
(Padoan & Nordlund 11)

multi-density
(Hennebelle & Chabrier 11)

combined
(Federrath & Klessen 12)

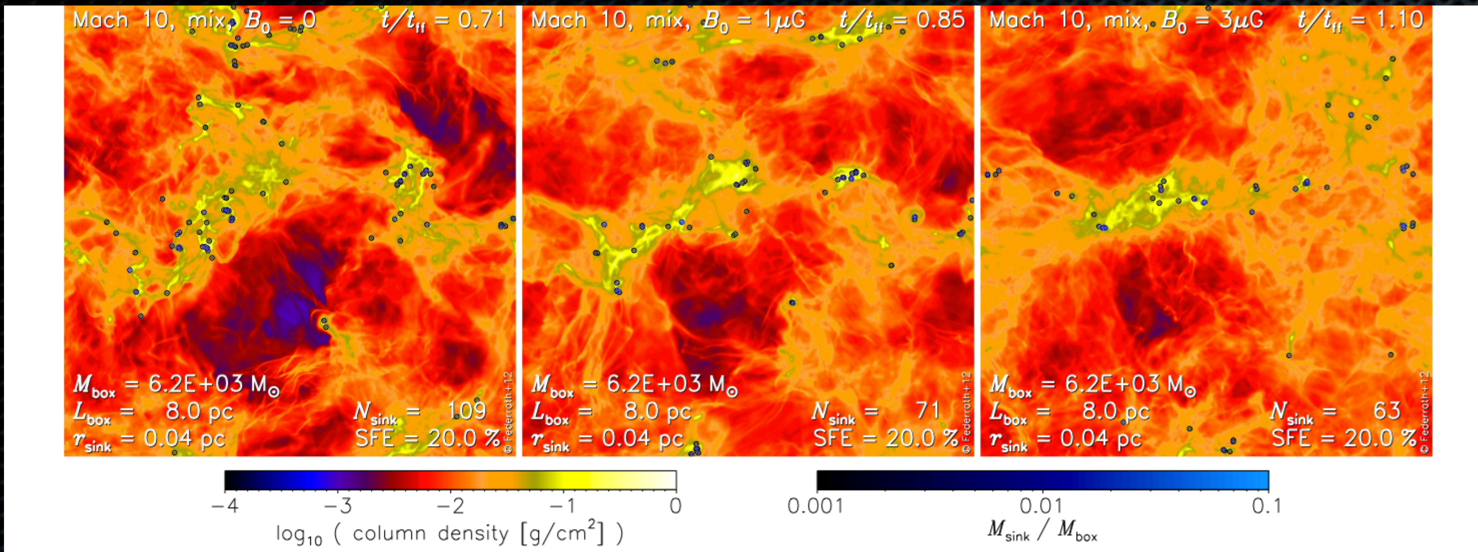

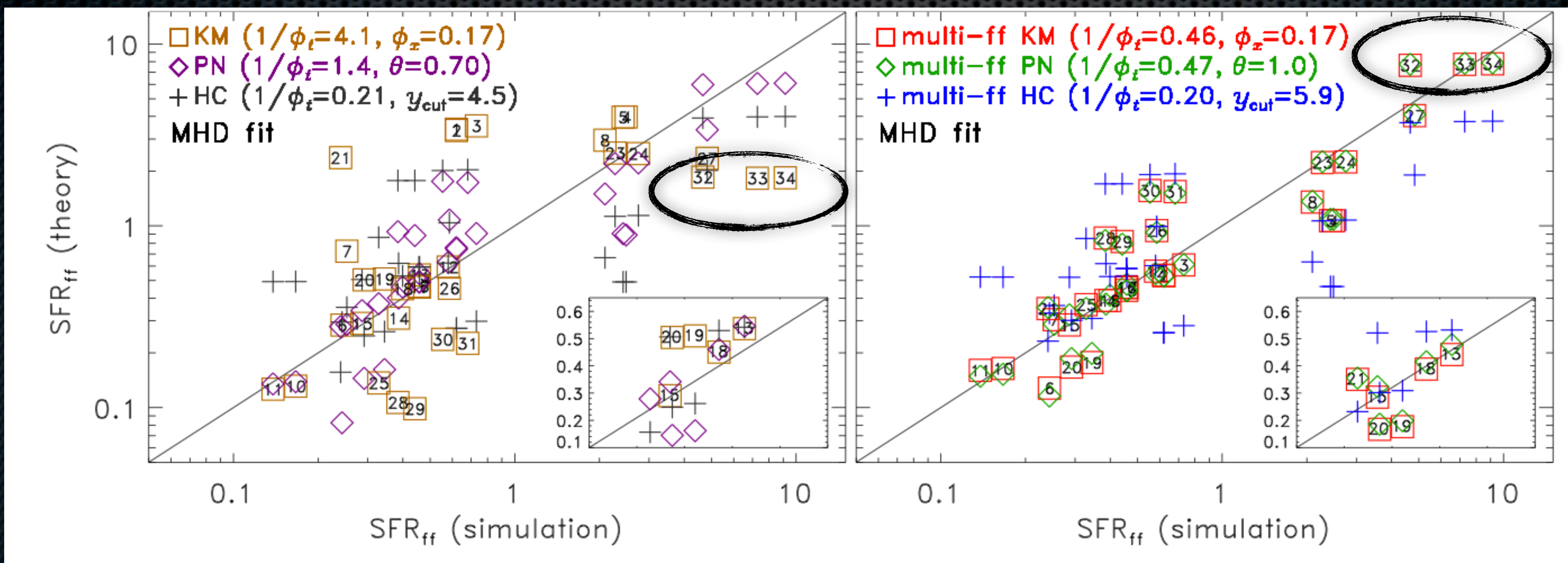

Federrath & Klessen 12

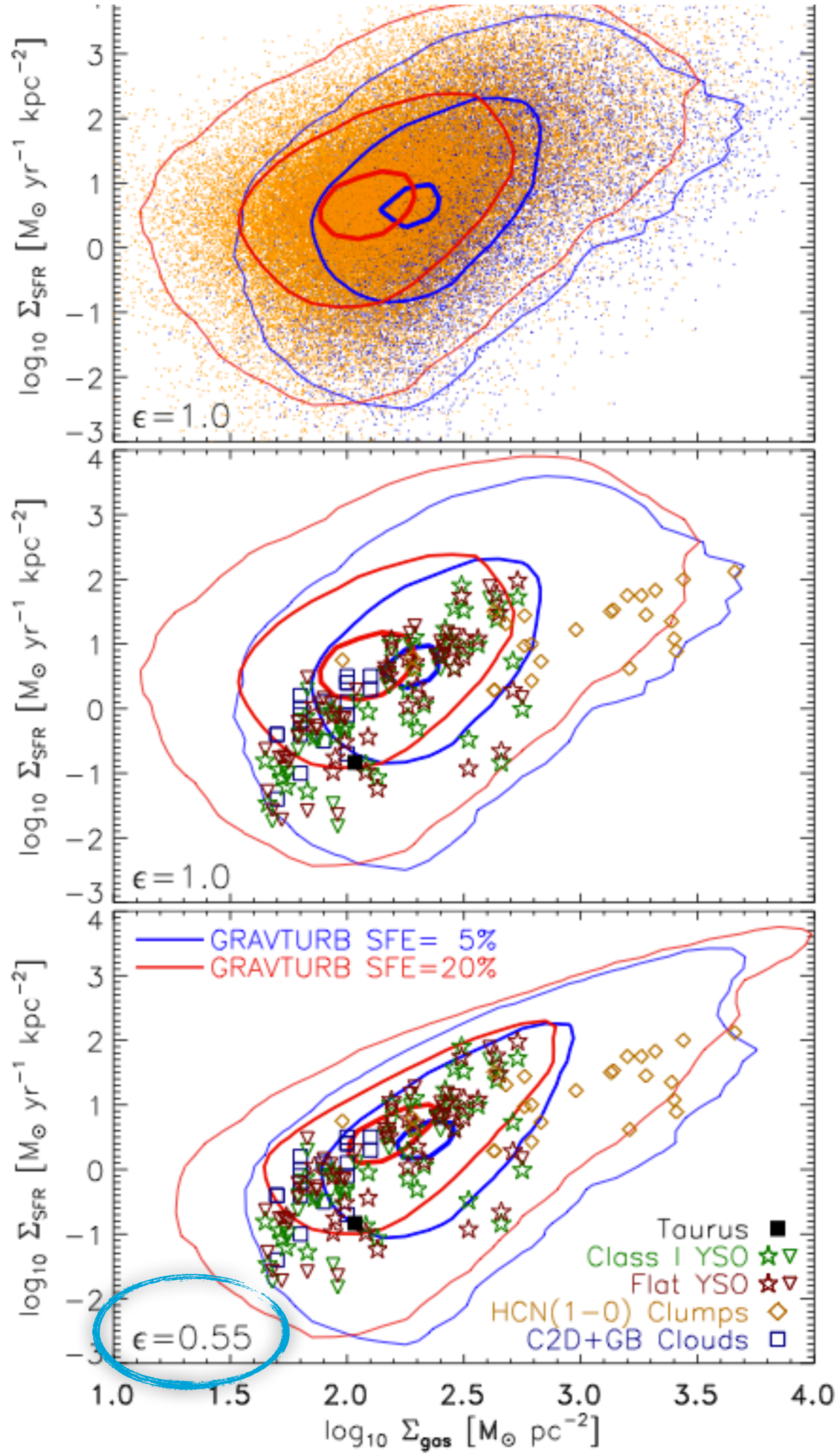

Federrath & Klessen 12
data from Heiderman + 10

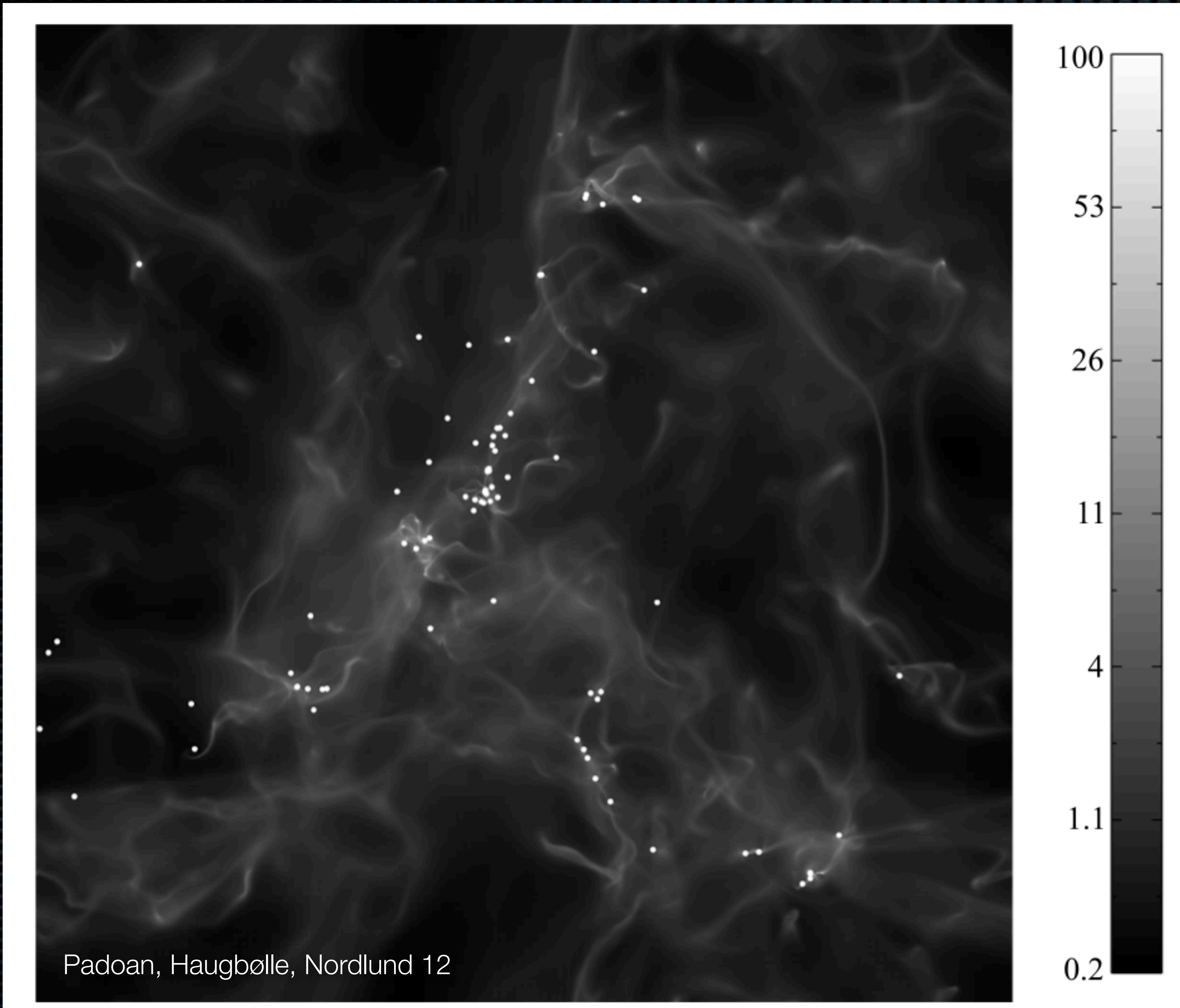

RAMSES AMR
128^3 base grid
+ 5 levels of
refinement
(4096^3 equiv.)

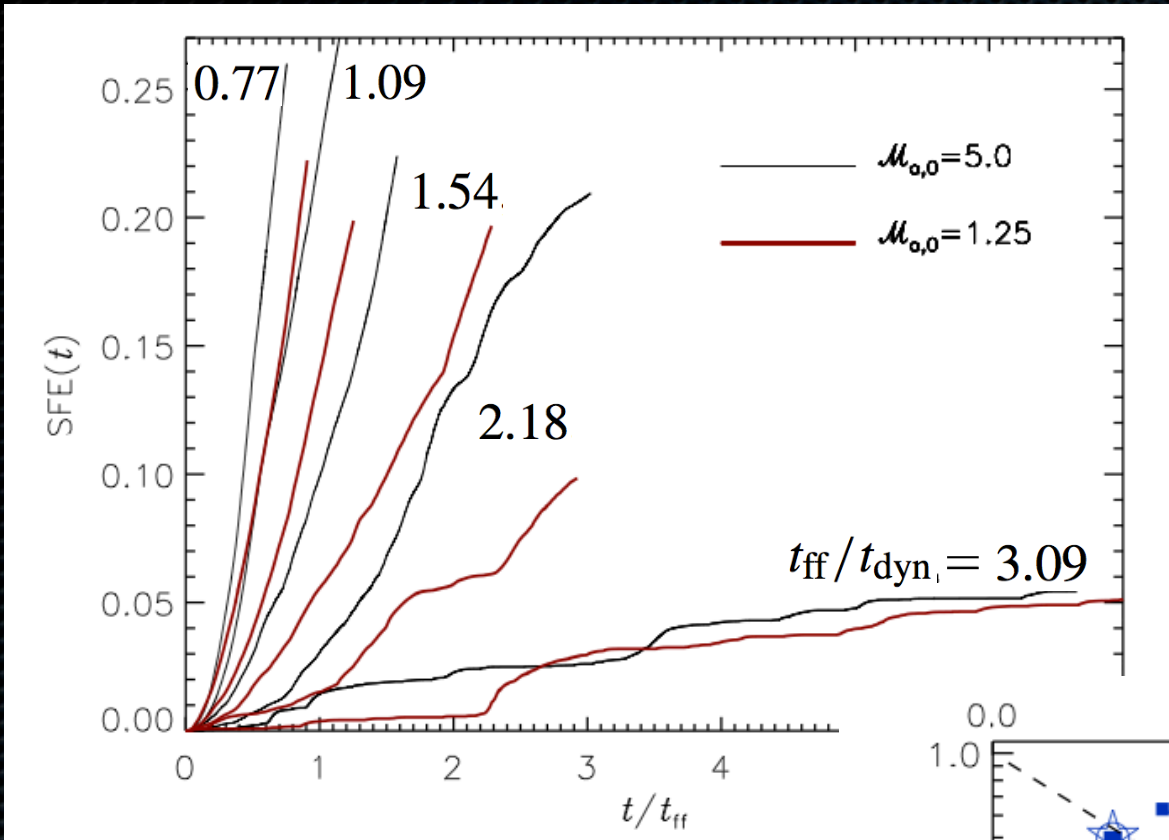

Padoan, Haugbølle, Nordlund 12

$$\epsilon_{ff} \approx \epsilon_{wind} \exp(-1.6\, t_{ff}/t_{dyn})$$

$$\epsilon_{wind} \approx 0.5$$

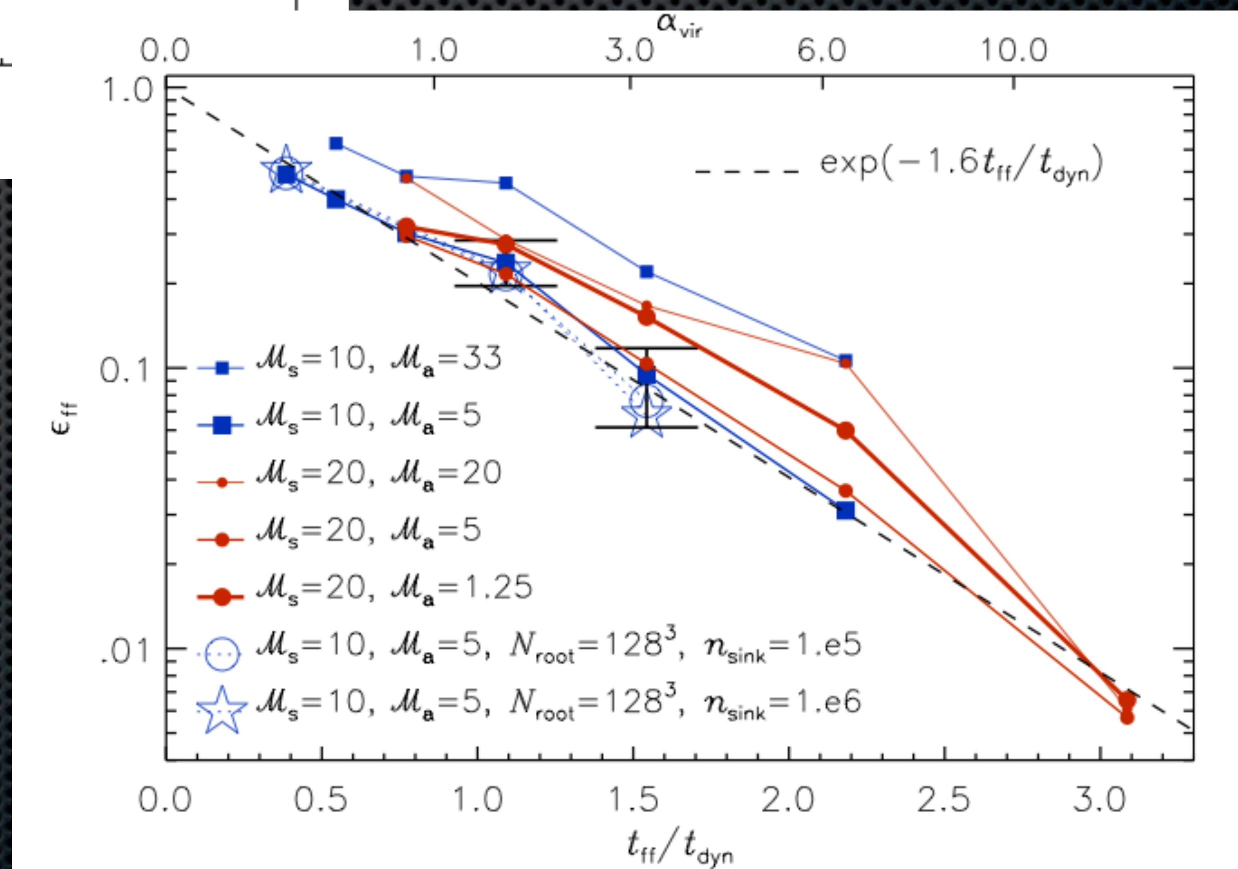

Massive star formation

NGC 3603, NASA, ESA, R. O'Connell (University of Virginia), F. Paresce (National Institute for Astrophysics, Bologna, Italy), E. Young (Universities Space Research Association/Ames Research Center), the WFC3 Science Oversight Committee, and the Hubble Heritage Team (STScI/AURA)

Radiation pressure can't prevent massive star formation (Krumholz + 09)...

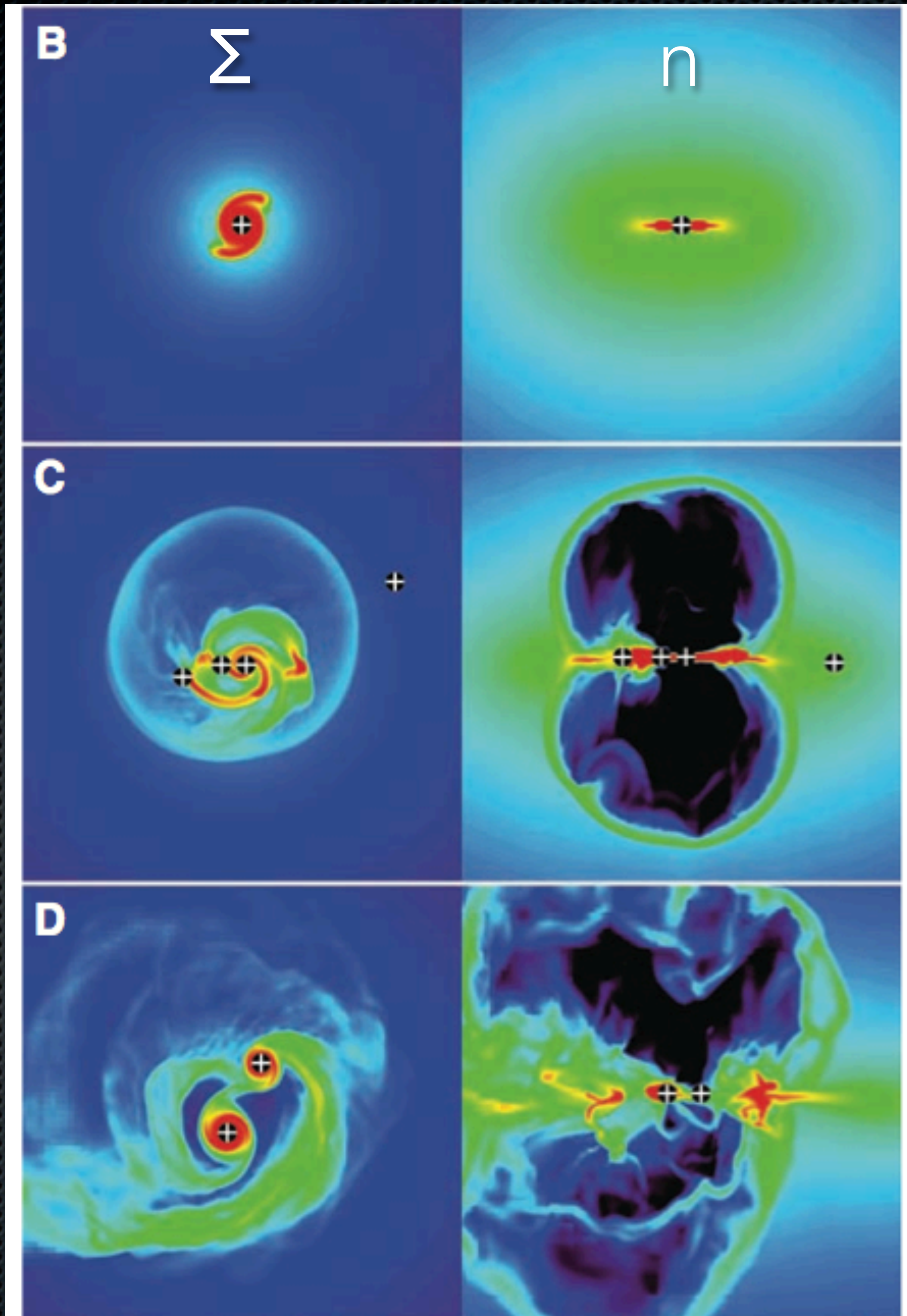

Radiation pressure can't prevent massive star formation

(Krumholz + 09)...

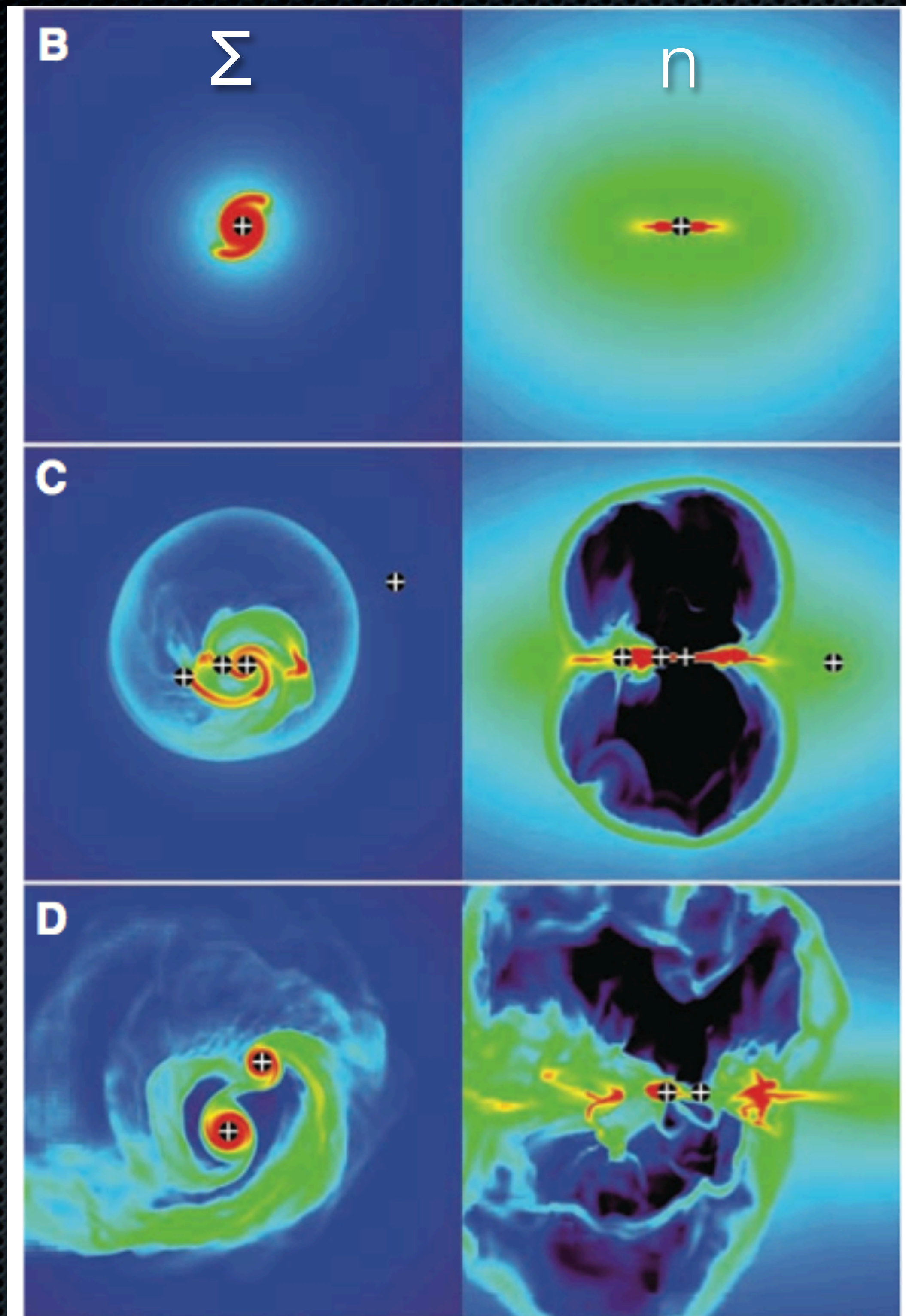

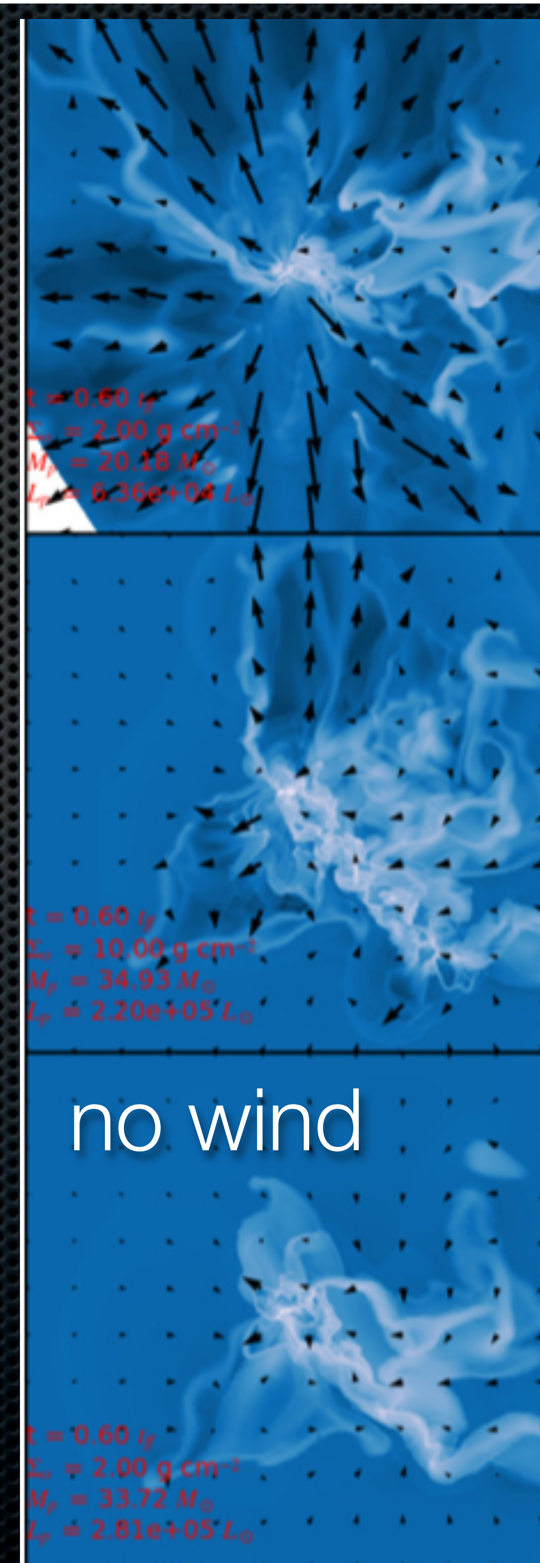

...particularly not when outflows occur

(Cunningham + 11)

What about ionization?

$$\left(\frac{\rho}{\rho_0}\right) = \left(\frac{r}{0.5\ \mathrm{pc}}\right)^{-3/2}$$

$$\rho_0 = 3 \times 10^{-20}\ \mathrm{g\ cm^{-3}}$$

$$M = 1000\ \mathrm{M_\odot}$$

$$\beta \equiv E_{rot}/E_{grav} = 0.05$$

solid body rotation

$$\Gamma = \Gamma_{\mathrm{ph}} + \Gamma_{\mathrm{st}} + \Gamma_{\mathrm{acc}}$$

photoionization — dust heating by star — accretion luminosity

$$\Lambda = \Lambda_{\mathrm{ml}} + \Lambda_{\mathrm{mol}} + \Lambda_{\mathrm{gd}}$$

metal lines — molecules — dust

FLASH adaptive mesh refinement (Fryxell 00)

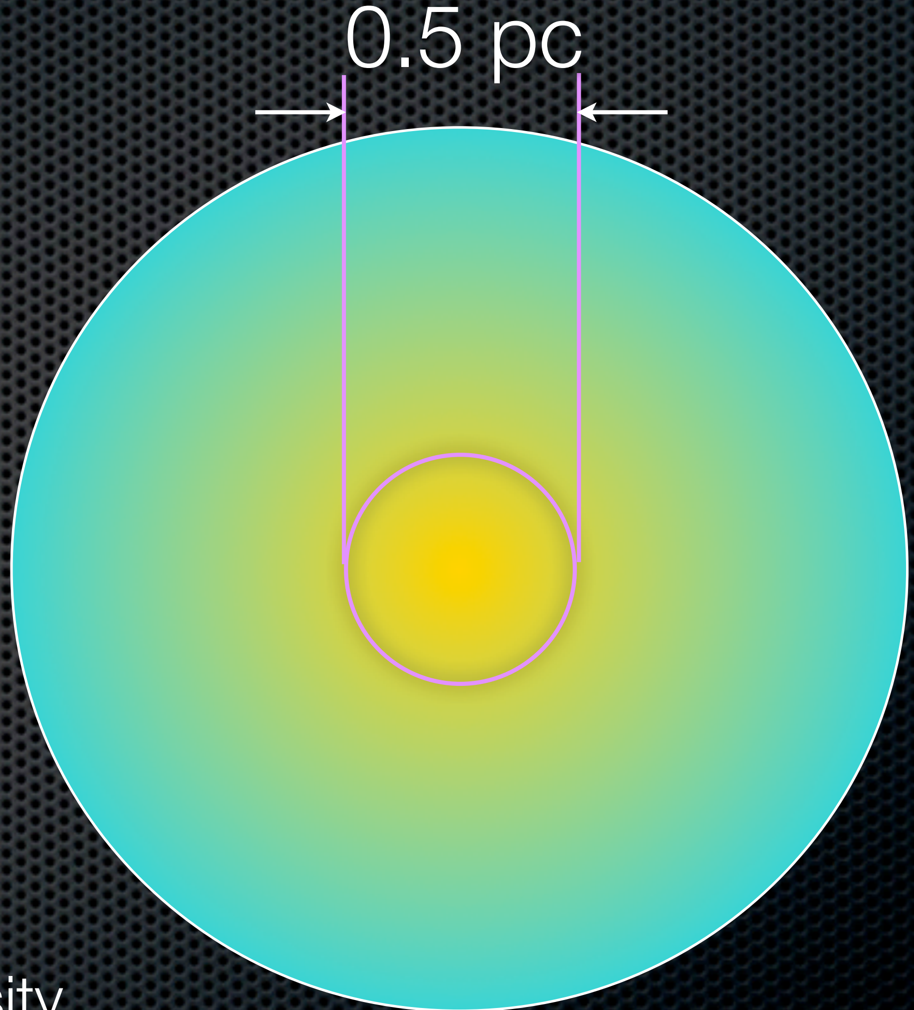

sink particles, ionization along hybrid characteristics

(Rijkhorst + 06; modified to allow higher resolution)

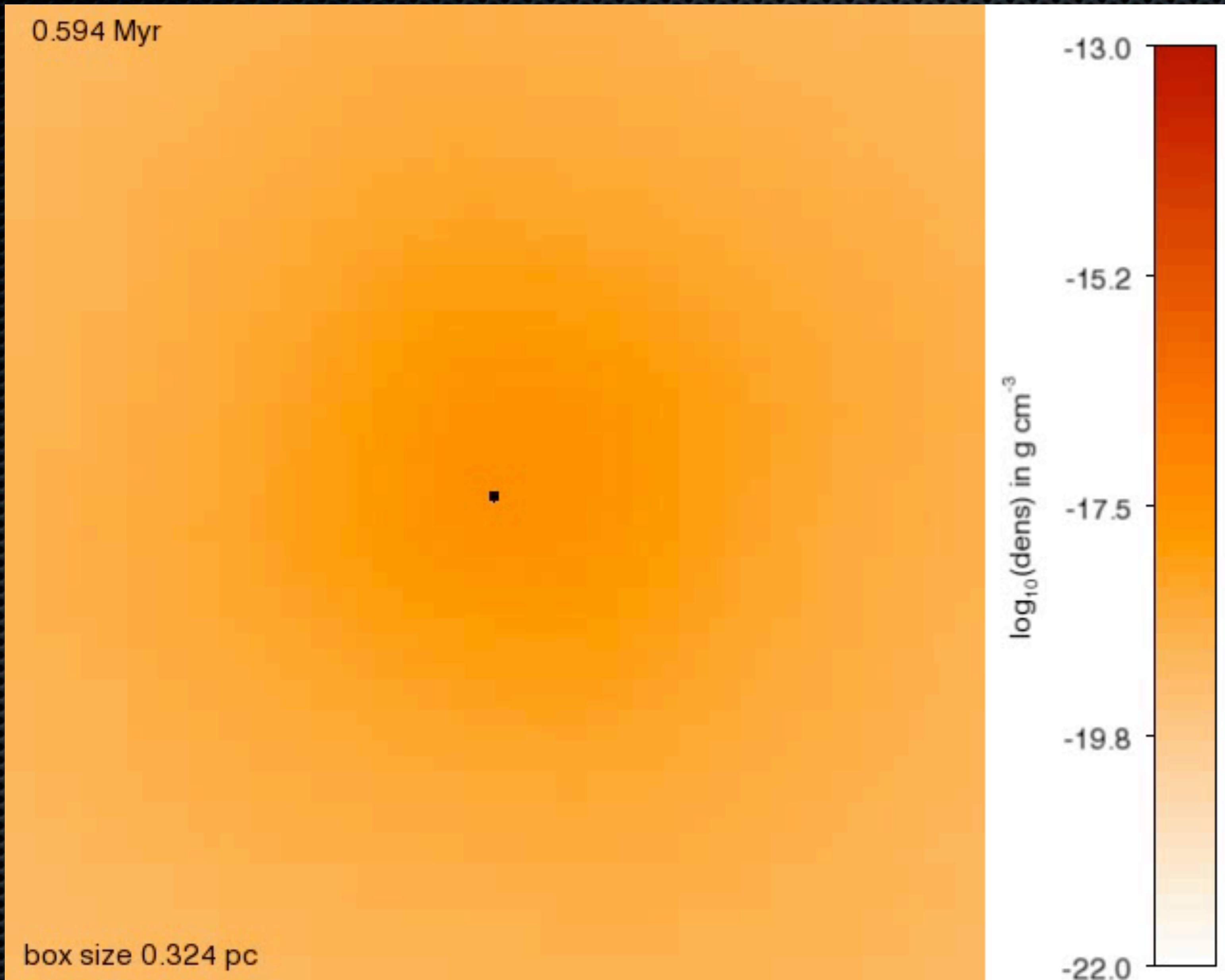
0.594 Myr
box size 0.324 pc
-13.0
-15.2
-17.5
-19.8
-22.0
log10(dens) in g cm-3
Peters+ 10a

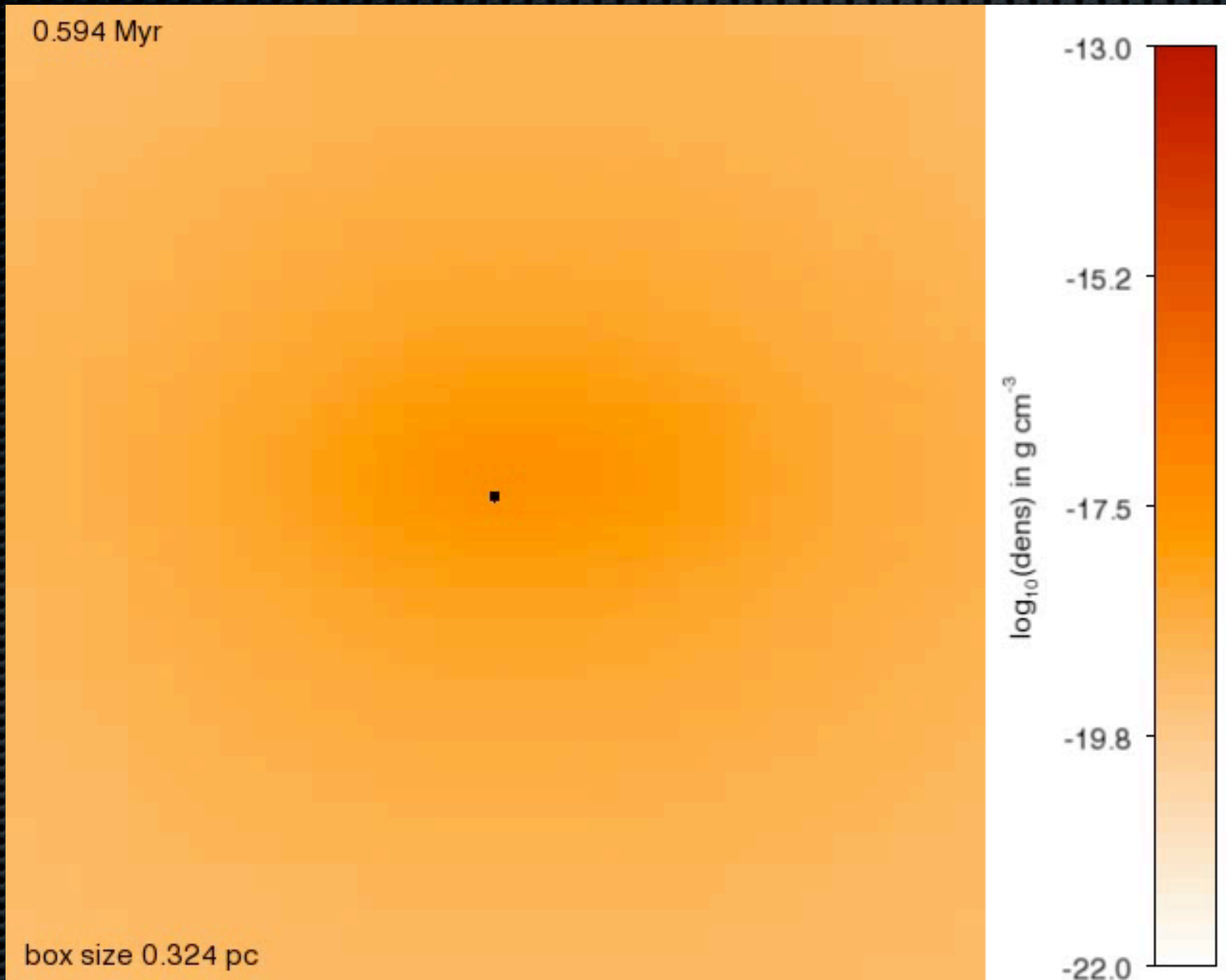
0.594 Myr
box size 0.324 pc
-13.0
-15.2
-17.5
-19.8
-22.0
log10(dens) in g cm-3

Peters+ 10a

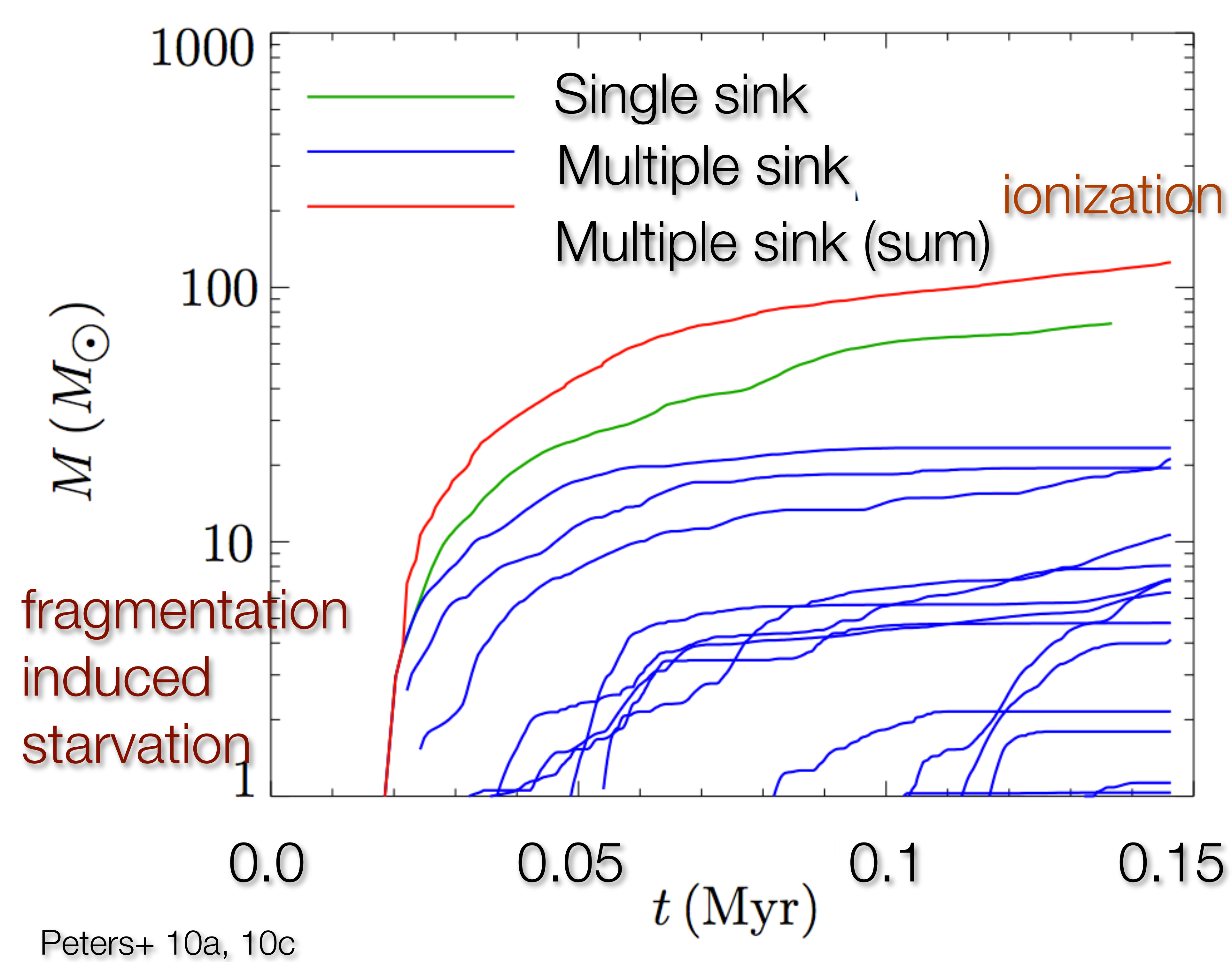
1000
100
10
1
Single sink
Multiple sink
Multiple sink (sum)
ionization
fragmentation
induced
starvation
$M\ (M_{\odot})$
0.0
0.05
0.1
0.15
t (Myr)
Peters+ 10a, 10c

Ultracompact H II Region live too long and have a variety of shapes.

- Radio continuum sources with r < 0.1 pc, EM > 10^7 pc cm^{-6}. Probably most easily observed consequences of ionizing feedback.

- Lifetime problem: if every UC H II region seen surrounds an OB star, UC H II lifetime is 10^5 yr, but dynamical ages are only 10^4 yr

- Morphologies: What explains wide variety of observed morphologies?

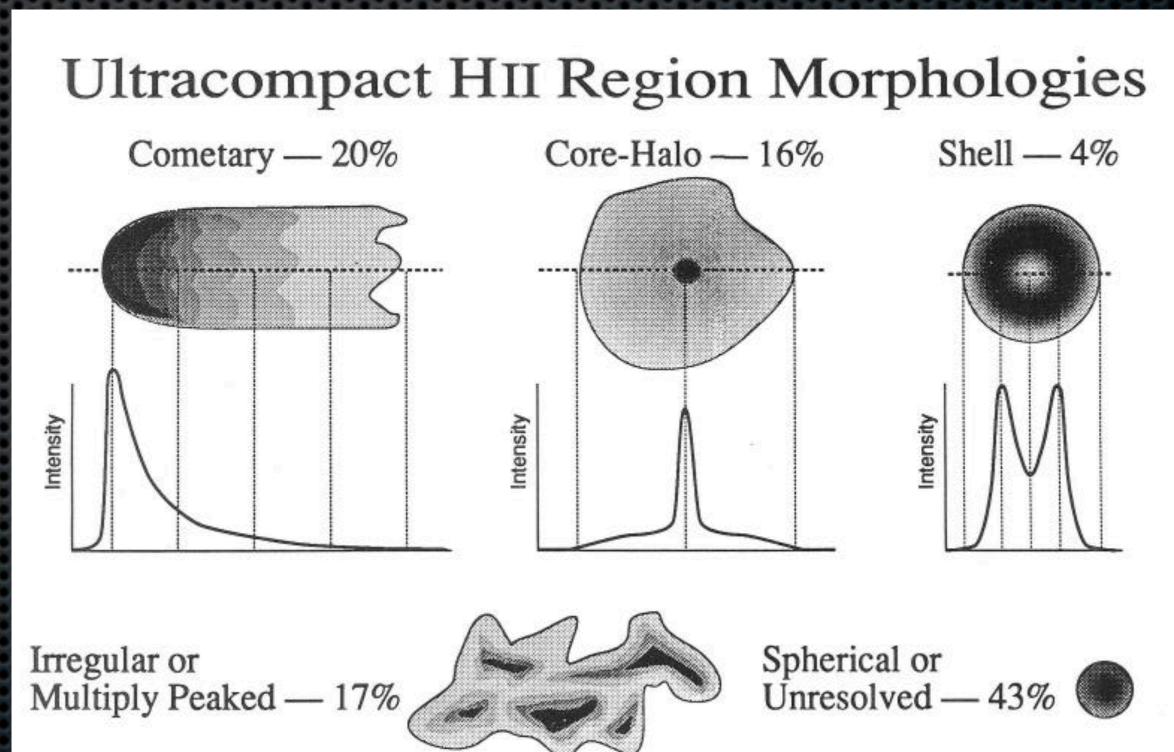

Wood & Churchwell 1989

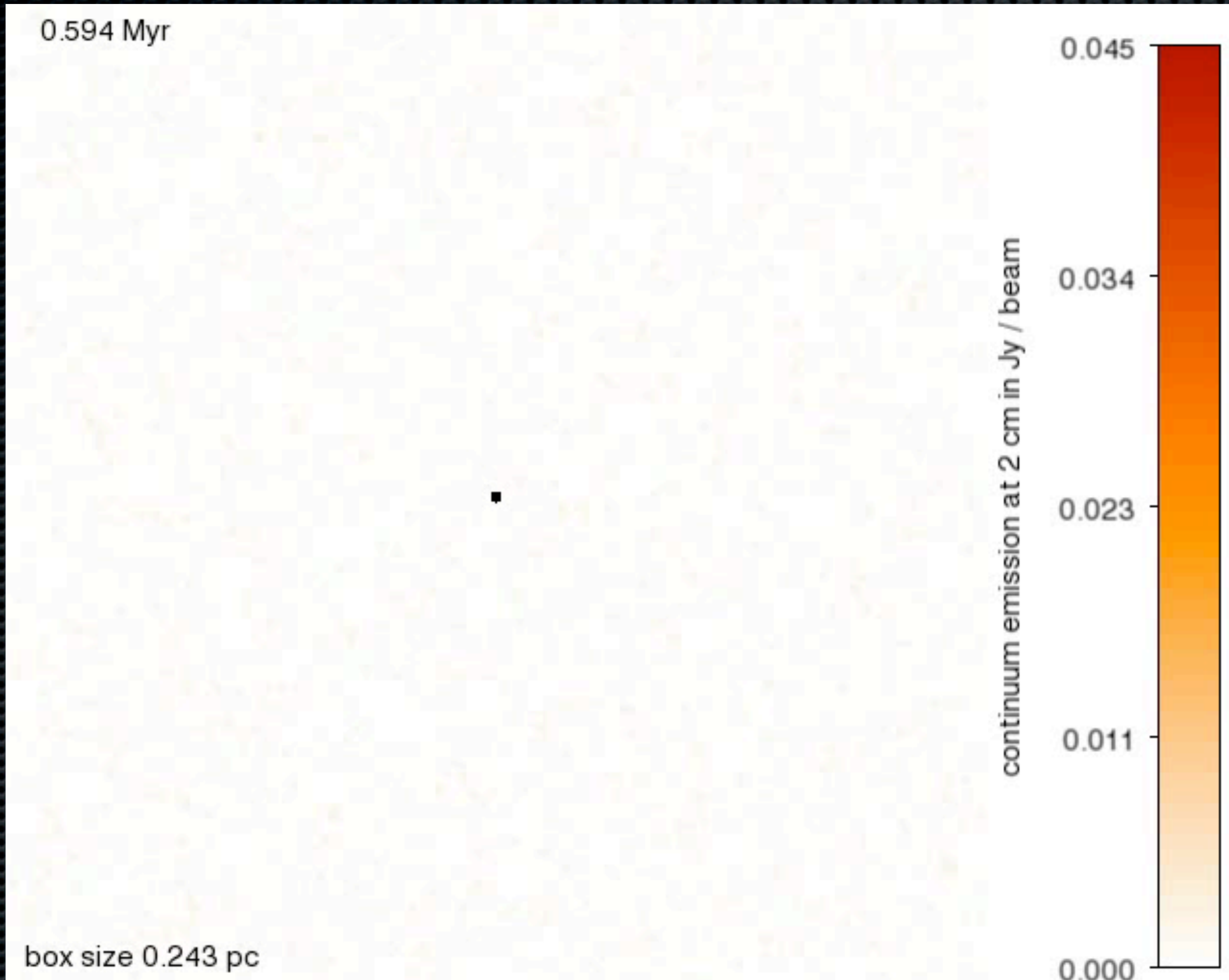

Peters+ 10a, 10b,
Galván-Madrid 11

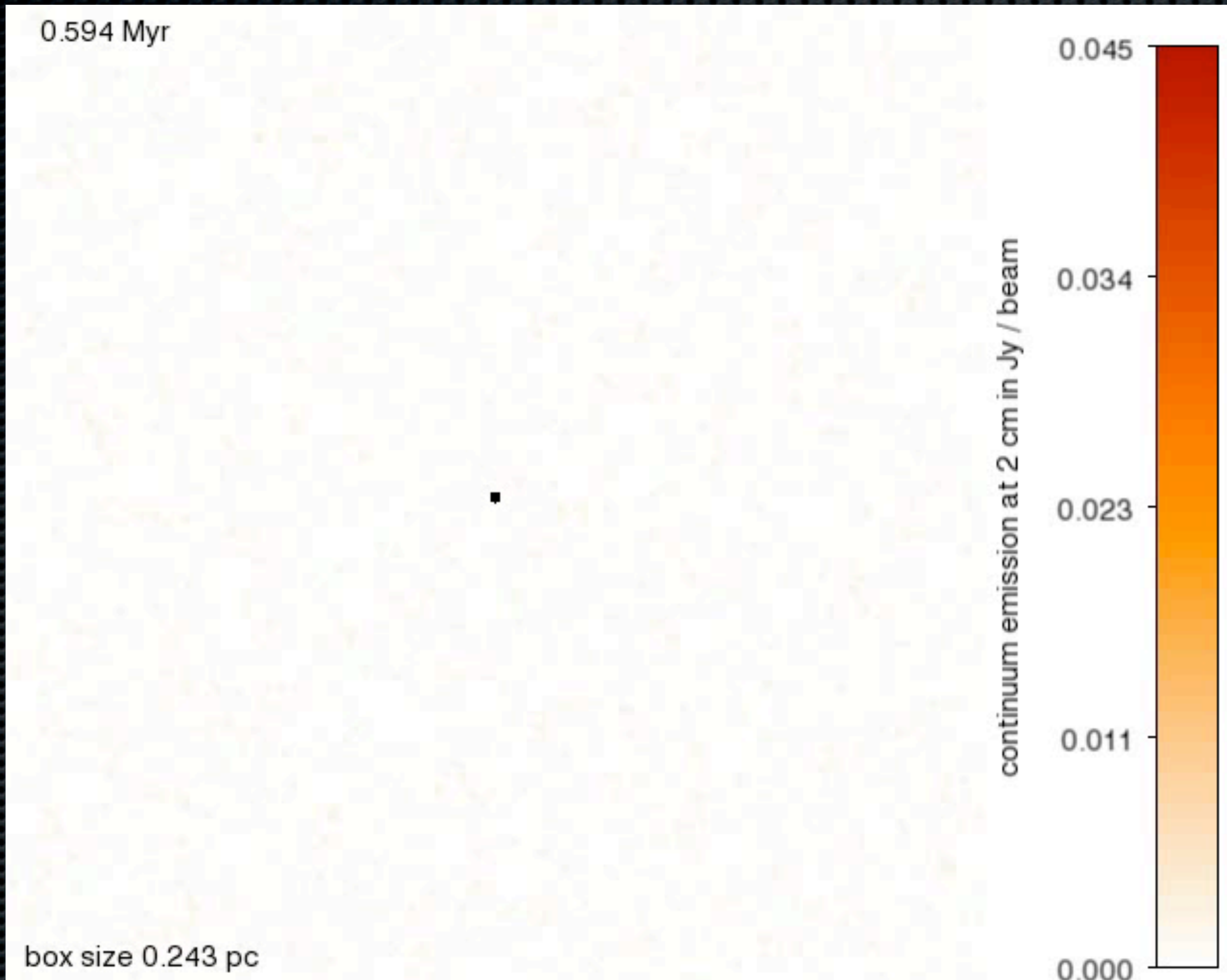

Peters+ 10a, 10b,
Galván-Madrid 11

Peters+ 10b

Table 3

Percentage Frequency Distribution of Morphologies

Type	WC89	K94	Single sink	Multiple sink
Spherical/Unresolved	43	55	19	60 ± 5
Cometary	20	16	7	10 ± 5
Core-halo	16	9	15	4 ± 2
Shell-like	4	1	3	5 ± 1
Irregular	17	19	57	21 ± 5

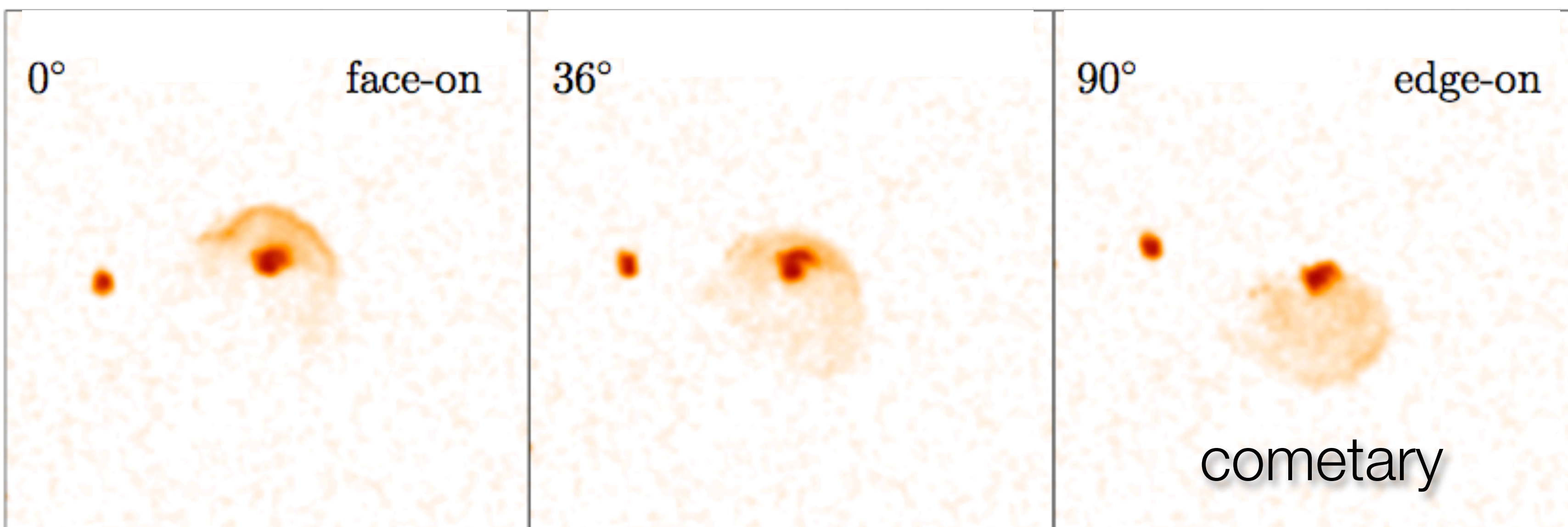

Peters+ 10b

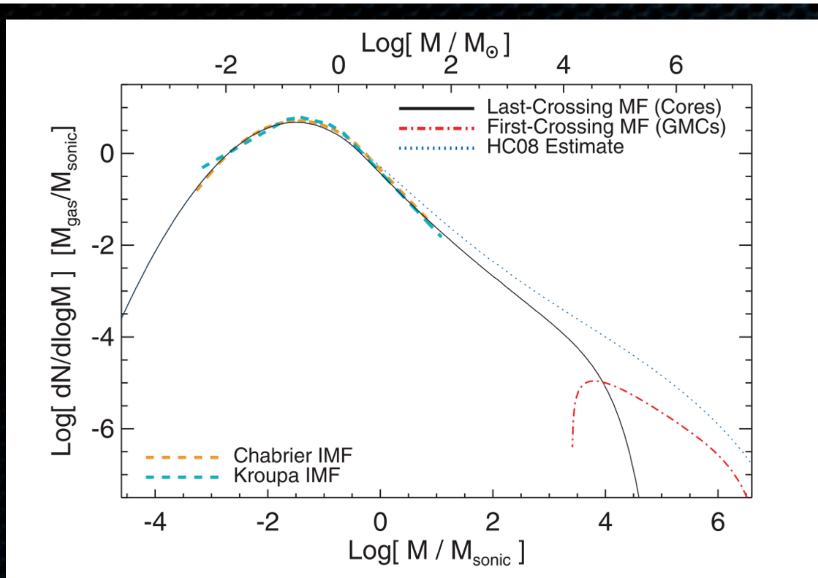

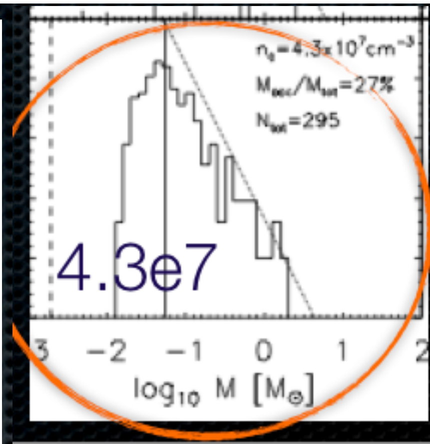

Conclusions